BULLETIN OF THE EARTHQUAKE
RESEARCH INSTITUTE
Vol. 45 (1967), pp. 91-136

8. A Long Wave around a Breakwater (Case of Perpendicular Incidence) [I].

By Takao MOMOI,

Earthquake Research Institute.

(Read Dec. 27, 1966.—Received Dec. 27, 1966.)

Abstract

In this paper, a theory of long waves around a breakwater is introduced by use of the method of the buffer domain, the behaviors of the waves thereabouts being elucidated with the aid of an electronic computer. Among the obtained results, the most conspicuous feature is an appearance of the reflected waves which produce a maximum wave height exceeding twice the amplitude of the incident waves in the nearby part of the mouth of a breakwater, causing a rotation of waves as a complementary flow.

Other than the approximated theories developed so far, the boundary conditions at the rigid walls of two breakwater wings are satisfied rigorously in the theory established in this paper (by use of the method of the buffer domain).

1. Introduction

When a train of periodic waves invades a gap of a breakwater, miscellaneous effects of a breakwater upon invading waves are expected. This problem has already been treated, theoretically and experimentally by many authors[1),2),3),4)], their studies having been carried out on the basis of approximated theory devised from Sommerfeld's diffraction theory which was established for light diffraction by a single semi-infinite plate.[5)] In the studies[1),2),3),4)] cited above, a problem of a gap of a breakwater is treated by superposition of two wings of plates, one of which

1) W. G. PENNY, and A. T. PRICE, "Diffraction of sea waves by breakwaters", *Directorate, Misc. Weapons Development Technical History* 26, *Artificial Harbours, Sec. 3D*, 1944.

2) J. A. PUTNAM, and R. S. ARTHUR, "Diffraction of water waves by breakwaters", *Trans. Amer. Geophys. Union*, **29** (1948), 481.

3) K. MOGI, *Bull. Earthq. Res. Inst.*, **34** (1956), 267.

4) Frank L. BLUE, Jr. and J. W. JOHNSON, *Trans. Amer. Geophys. Union*, **30** (1949), 705.

5) G. WOLFSOHN, *Handbuch der Physik XX, Kapitel 7.*

extends to the right and the other to the left, neglecting the influence of a wing upon the waves diffracted by another wing or suitably approximating such effect. But if a gap of a breakwater is small, the above approximation might not be possible, since it is expected that a wing has not a little influence upon the diffracted waves from another wing. Hence, the numerical calculations of the theory developed in this paper have been made for the waves in the range of small kd (k: a wave number of the incident waves, d: a half width of a gap of a breakwater).

In the present purview, a general theory is developed on the basis of a long wave equation in Section 2 by use of *the method of the buffer domain* which has been introduced first by the author, numerical computations and their discussions being done in subsequent sections.

In the nearby part of a mouth of a breakwater, vortices of water are, in general, produced with inertia terms of an equation of motion supposedly outweighing the term of acceleration as a result of an increase in velocity of water particles, so that the applicability of a long wave equation becomes very dubious to this problem.

Although there exist the above-mentioned circumstances, a rigorous treatment of this problem based on a long wave equation is considered to be still highly significant. Since such rigorous treatment has not as yet been made considerable insight would, if carried out, be brought the problem of the effects of a breakwater with a small gap upon long waves including tsunamis.

2. Theory

In this section, a development of a general theory is described.

2,1. The Geometry of a Used Model.

Referring to Fig. 1, a breakwater is assumed to be thin plate with infinitesimal thickness, which is located in the open sea so as to separate the waters into two semi-infinite regions. The origin of the coordinate is centered in the midpoint of the mouth of a breakwater, of which the breadth is taken as $2d$, a breakwater being situated on the x-axis of the Cartesian coordinate.

The depth of the sea is assumed to be uniform throughout an entire portion of the domains of water. Then a train of periodic waves is propagated perpendicular to the breakwater, which is stated by

$$\zeta_0 \exp(-i\omega t - iky)\,, \tag{1}$$

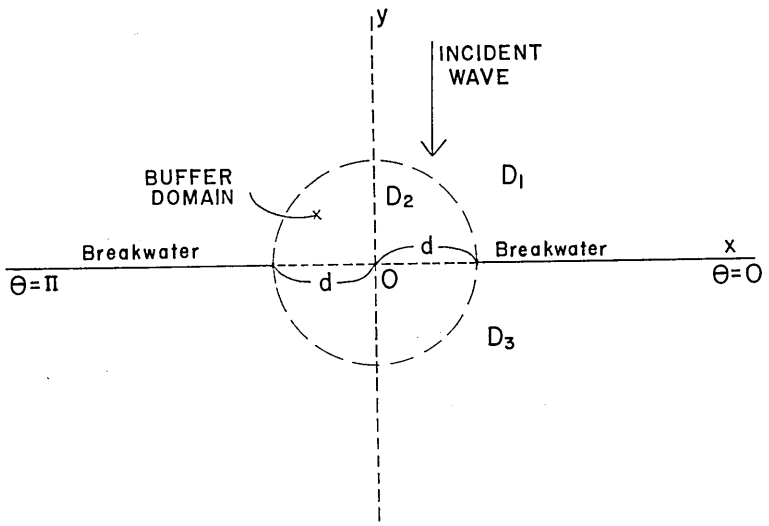

Fig. 1. Geometry of a used model.

where

ζ_0 : an amplitude of the incident waves,
ω : an angular frequency of the incident waves,
k : a wave number of the incident waves,
t : a variable of time,
y : the y-component of the Cartesian coordinate.

In the above expression, only the real part has a physical meaning, following the usual convention.

2,2. A Governing Equation and Boundary Conditions.

An equation employed in the present article is a long wave equation, i.e.,

$$\frac{1}{c^2}\frac{\partial^2\zeta}{\partial t^2}=\frac{\partial^2\zeta}{\partial x^2}+\frac{\partial^2\zeta}{\partial y^2}\,, \tag{2}$$

where

ζ : an elevation of water surface,
c : a velocity of a long wave.

For the case of periodic waves, the equation (2) is reduced to

$$\frac{\partial^2\zeta'}{\partial x^2}+\frac{\partial^2\zeta'}{\partial y^2}+k^2\zeta'=0\,. \tag{3}$$

Then k is related with ω through the relation $\omega=kc$.

Using the polar coordinate, (3) is written, as an another expression, as follows:—

$$\frac{\partial^2\zeta'}{\partial r^2}+\frac{1}{r}\frac{\partial\zeta'}{\partial r}+\frac{1}{r^2}\frac{\partial^2\zeta'}{\partial\theta^2}+k^2\zeta'=0\,, \tag{4}$$

where r and θ are the components of the polar coordinate.

In the equations (3) and (4), ζ' stands for the quantity of ζ from which a time factor $\exp(-i\omega t)$ is excluded. For the sake of simplicity, the prime of ζ' is omitted in what follows, unless otherwise stated.

As far as the boundary condition is concerned, we have the condition at the rigid wall of the breakwater expressed as

$$\left.\begin{aligned}&\frac{\partial\zeta}{\partial y}=0 \qquad (y=0\,;\ |x|>d)\\ \text{or}\\ &\frac{\partial\zeta}{\partial\theta}=0 \qquad (\theta=0 \text{ and } \pi\,;\ |x|>d)\,.\end{aligned}\right\} \tag{5}$$

The above condition denotes that the flux of water vanishes at the wall.

2,3. A principle of the Analysis.

A principle of the analysis used in the present work is a method of the buffer domain which was introduced firstly by the author. This method has already been employed in the analysis of the problems on long waves in canals of several kinds of forms[6)-9)], in the vicinity of an estuary[10),11)], and so forth. This method is recapitulated hereunder.

When two domains are connected through a small region, the former of which is named a "non-buffer domain" and the latter a "buffer domain" (see Fig. 2), the solutions in the non-buffer domains are firstly expressed by a series of functions with orthogonal properties, while the solution in the buffer domain may be described in an appropriate form which not always necessitates the nature of orthogonality of the expression.

6) T. MOMOI, *Bull. Earthq. Res. Inst.*, **40** (1962), 719.
7) T. MOMOI, *Bull. Earthq. Res. Inst.*, **42** (1964), 449.
8) T. MOMOI, *Bull. Earthq. Res. Inst.*, **43** (1965), 745.
9) T. MOMOI, *Bull. Earthq. Res. Inst.*, **44** (1966), 121.
10) T. MOMOI, *Bull. Earthq. Res. Inst.*, **43** (1965), 291.
11) T. MOMOI, *Bull. Earthq. Res. Inst.*, **43** (1965), 459.

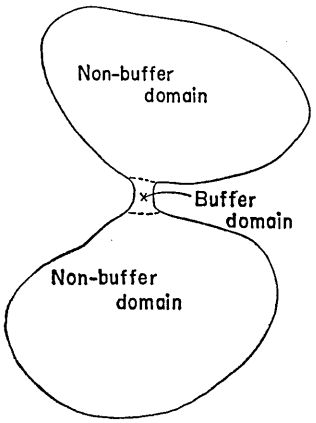

Fig. 2. Figurative explanation of buffer and non-buffer domains.

Then connecting the above solutions by use of the boundary conditions between the adjacent domains and exposing each mode of the expressions by virtue of the orthogonalities of serial solutions, we can arrive at infinite simultaneous equations. Hereafter, approximating the expression in the buffer domain appropriately, the above-mentioned simultaneous equations are reduced to the forms which are approachable by direct analysis or numerical procedures. In this way, all the unknowns in the buffer and non-buffer domains begin to be analytically or numerically known quantities.

Finally, substituting these known values into the formal expressions in each domain, the behaviors of the waves in all domains are elucidated analytically or through numerical calculations.

2,4. Formal Solutions.

In this section, formal solutions of the waves are presented.

In our model, all the domains are separated into three parts, that is to say, (referring to Fig. 1)

the domain D_1 is a region such that $0 \leqq \theta \leqq \pi$ and $d \leqq r$,

the domain D_3 is a region such that $\pi \leqq \theta \leqq 2\pi$ and $d \leqq r$,

and

the domain D_2 is a circular region defined by $0 \leqq r < d$.

In the above three domains, the first two are non-buffer domains and the last one the buffer domain mentioned in *2,3*.

To begin with, the formal solution in the domain D_1 is obtained.

When a train of periodic waves stated by

$$\zeta_0 \exp(-iky)$$

is given, a particular solution of the equation (3) satisfying the boundary condition (5) is

$$2\zeta_0 \cos ky\,. \tag{6}$$

This solution implies standing waves caused at the straight breakwater.

If one obtains a general solution of the equation (3) or (4) under

the condition (5), the formal solution which determines the wave motion in the domain D_1 is described by a sum of the above general solution and a particular solution (6). And from a physical point of view, such a general solution is required to be scattered waves leaving from the mouth of a breakwater. The last requirement is fulfilled if the first kind of the Hankel function is employed.

Suppose that the domain D_1 is extended hypothetically to the lower half region so as to be symmetrical with respect to the x-axis in Fig. 1, we can express the scattered outgoing waves as follows:—

$$\sum_{m=0}^{\infty} \zeta_1^{(m)} H_m^{(1)}(kr) \cos m\theta$$

where $\zeta_1^{(m)}$ $(m=0, 1, 2,\cdots)$ are the unknowns to be determined by the conditions between the adjacent domains. The satisfaction of the boundary condition (5) then follows as a necessary consequence.

Further, taking account of a symmetry of the phenomenon with respect to the y-axis, this expression is reduced to

$$\sum_{m=0}^{\infty} \zeta_1^{(2m)} H_{2m}^{(1)}(kr) \cos 2m\theta \,. \tag{7}$$

Now the formal solution in the domain D_1 becomes from (6) and (7)

$$\zeta_1 = 2\zeta_0 \cos ky + \sum_{m=0}^{\infty} \zeta_1^{(2m)} H_{2m}^{(1)}(kr) \cos 2m\theta \,, \tag{8}$$

where ζ_1 is the height of waves in the domain D_1.

In like manner, the formal solution in the domain D_3 is obtained by an extension of the domain D_3 to the upper half plane in Fig. 1 in such a way that an entire region begins to be symmetrical with respect to the x-axis. That is to say,

$$\zeta_3 = \sum_{m=0}^{\infty} \zeta_3^{(2m)} H_{2m}^{(1)}(kr) \cos 2m\theta \,, \tag{9}$$

where ζ_3 and $\zeta_3^{(2m)}$ $(m=0, 1, 2,\cdots)$ are a height of waves and unknown factors respectively in the domain D_3, and where modes relevant to $\cos(2m+1)\theta$ $(m=0, 1, 2,\cdots)$ are excluded because of the symmetry of the problem for the y-axis.

This expression, of course, satisfies the condition (5) at the breakwater.

Let us finally consider the solution in the domain D_2 or buffer domain.

In this area, a form of the Fourier-Bessel expansion is taken. Allowing for the symmetry of the phenomenon with respect to the y-axis, the formal solution becomes as follows:—

$$\zeta_2=\sum_{m=0}^{\infty}\{\bar{\zeta}_2^{(2m)}J_{2m}(kr)\cos 2m\theta+\zeta_2^{(2m+1)}J_{2m+1}(kr)\sin(2m+1)\theta\}\,, \tag{10}$$

where $\bar{\zeta}_2^{(2m)}$, $\zeta_2^{(2m+1)}$ $(m=0, 1, 2,\text{- - -})$ and ζ_2 are unknown factors and a wave height in the domain D_2.

We have now arrived at the state which makes possible a formation of infinite simultaneous equations by use of orthogonalities of serial solutions in the non-buffer domains D_1 and D_3.

2,5. Infinite Simultaneous Equations.

In this section, an infinte number of simultaneous equations are derived from the formal solutions (8)-(10) and the conditions between the adjacent domains. Such conditions are as follows:—

$$\left.\begin{aligned}\zeta_2&=\zeta_1\\ \frac{\partial\zeta_2}{\partial r}&=\frac{\partial\zeta_1}{\partial r}\end{aligned}\right\}\ \text{for}\ (r=d\,,\ 0<\theta<\pi) \tag{11}$$

and

$$\left.\begin{aligned}\zeta_2&=\zeta_3\\ \frac{\partial\zeta_2}{\partial r}&=\frac{\partial\zeta_3}{\partial r}\end{aligned}\right\}\ \text{for}\ (r=d\,,\ \pi<\theta<2\pi)\,. \tag{12}$$

The first relations of (11) and (12) stand for the continuities of wave heights and the second ones the continuities of velocities of water particles.

Substituting the formal solutions (8) and (10) into (11), and applying the operators of the orthogonal functions in the domain D_1, i.e.

$$\int_0^{\pi}\cos 2n\theta d\theta\ \ (n=0, 1, 2,\text{- - -}) \tag{13}$$

to them, we have the following:—

$$\begin{Bmatrix}J_{2n}(kd)\\ J'_{2n}(kd)\end{Bmatrix}\bar{\zeta}_2^{(2n)}+\frac{2}{\pi}\varepsilon_n\sum_{m=0}^{\infty}\frac{(2m+1)}{(2m+1)^2-(2n)^2}\begin{Bmatrix}J_{2m+1}(kd)\\ J'_{2m+1}(kd)\end{Bmatrix}\zeta_2^{(2m+1)}$$

$$-\begin{Bmatrix} H_{2n}^{(1)}(kd) \\ H_{2n}^{(1)\prime}(kd) \end{Bmatrix} \zeta_1^{(2n)} = 2\varepsilon_n \begin{Bmatrix} J_{2n}(kd) \\ J_{2n}'(kd) \end{Bmatrix} \zeta_0 , \tag{14}$$

where $n=0, 1, 2,---$,

$$\varepsilon_n = \begin{Bmatrix} 1 \text{ for } n=0 , \\ 2 \text{ for } n \geqq 1 , \end{Bmatrix} \tag{15}$$

and where the quantities in the wavy brackets are taken in the same order. On the occasion of the above reductions, the expansion[12] of $\cos ky$ by the Fourier-Bessel series is used, i.e.

$$\cos ky = \sum_{m=0}^{\infty} \varepsilon_m J_{2m}(kr) \cos 2m\theta . \tag{16}$$

In like manner, after substituting (9) and (10) into (12), the operators

$$\int_{\pi}^{2\pi} \cos 2n\theta d\theta \quad (n=0, 1, 2,---) \tag{17}$$

are applied to them. We have then the following equations:—

$$\begin{Bmatrix} J_{2n}(kd) \\ J_{2n}'(kd) \end{Bmatrix} \zeta_2^{(2n)} - \frac{2}{\pi} \varepsilon_n \sum_{m=0}^{\infty} \frac{(2m+1)}{(2m+1)^2-(2n)^2} \begin{Bmatrix} J_{2m+1}(kd) \\ J_{2m+1}'(kd) \end{Bmatrix} \zeta_2^{(2m+1)}$$

$$-\begin{Bmatrix} H_{2n}^{(1)}(kd) \\ H_{2n}^{(1)\prime}(kd) \end{Bmatrix} \zeta_3^{(2n)} = 0 , \tag{18}$$

where the quantities in the wavy brackets are taken in the same order and $n=0, 1, 2,---$.

Comparing the applied operators (13) and (17), the range of the integrations is from 0 to π for the former and π to 2π for the latter, though the other factors are completely identical to each other.

As infinite simultaneous equations for numerical calculations, we might employ the forms given in (14) and (18). But these equations are further reduced to more simplified forms in consideration of the capacity of used computer, stability of infinite simultaneous equations, efficiency of numerical calculations, convenience of a few interpretations of the behaviors of the waves around the mouth of a breakwater and so on.

12) S. MORIGUCHI, *et al.*, *Sūgaku Kōshiki III* (literally, *Mathematical Formula III*) (Iwanami Shoten, 1961), 211.

Setting down

$$\begin{Bmatrix} F_n \\ F_n' \end{Bmatrix} = \frac{2}{\pi} \varepsilon_n \sum_{m=0}^{\infty} \frac{(2m+1)}{(2m+1)^2-(2n)^2} \begin{Bmatrix} J_{2m+1}(kd) \\ J_{2m+1}'(kd) \end{Bmatrix} \zeta_2^{(2m+1)} \tag{19}$$

in (14) and transferring these quantities to the right-hand sides of the equations, (14) then becomes

$$\begin{Bmatrix} J_{2n}(kd) \\ J_{2n}'(kd) \end{Bmatrix} \bar{\zeta}_2^{(2n)} - \begin{Bmatrix} H_{2n}^{(1)}(kd) \\ H_{2n}^{(1)\prime}(kd) \end{Bmatrix} \zeta_1^{(2n)} = 2\varepsilon_n \begin{Bmatrix} J_{2n}(kd) \\ J_{2n}'(kd) \end{Bmatrix} \zeta_0 - \begin{Bmatrix} F_n \\ F_n' \end{Bmatrix}, \tag{20}$$

where the quantities in the wavy brackets of (20) are taken in the same order.

Solving the equations (20) in terms of $\bar{\zeta}_2^{(2n)}$ and $\zeta_1^{(2n)}$, the following are obtained as the solutions:—

$$\bar{\zeta}_2^{(2n)} = 2\varepsilon_n \zeta_0 + \frac{1}{\Delta} \{F_n H_{2n}^{(1)\prime}(kd) - F_n' H_{2n}^{(1)}(kd)\}, \tag{21}$$

and

$$\zeta_1^{(2n)} = \frac{1}{\Delta} \{F_n J_{2n}'(kd) - F_n' J_{2n}(kd)\}, \tag{22}$$

where

$$\Delta = J_{2n}'(kd) H_{2n}^{(1)}(kd) - J_{2n}(kd) H_{2n}^{(1)\prime}(kd). \tag{23}$$

Likewise, substituting (19) into (18) and solving the former in terms of $\bar{\zeta}_2^{(2n)}$ and $\zeta_3^{(2n)}$, we have

$$\bar{\zeta}_2^{(2n)} = \frac{1}{\Delta} \{F_n' H_{2n}^{(1)}(kd) - F_n H_{2n}^{(1)\prime}(kd)\} \tag{24}$$

and

$$\zeta_3^{(2n)} = \frac{1}{\Delta} \{F_n' J_{2n}(kd) - F_n J_{2n}'(kd)\}, \tag{25}$$

where Δ is the same as that described in (23).

From (21) and (24), the expression $\bar{\zeta}_2^{(2n)}$ is reduced to the following:—

$$\bar{\zeta}_2^{(2n)} = \varepsilon_n \zeta_0. \tag{26}$$

And also, from (22) and (25), the relation

$$\zeta_1^{(2n)} = -\zeta_3^{(2n)} \tag{27}$$

yields.

In (26) and (27), n is a non-negative integer extending from 0 to infinity.

Using (26) and (27), the infinite simultaneous equations (14) or (18) are reduced to the following series of simplified equations:—

$$\frac{2}{\pi}\varepsilon_n \sum_{m=0}^{\infty} \frac{(2m+1)}{(2m+1)^2-(2n)^2} \begin{Bmatrix} J_{2m+1}(kd) \\ J'_{2m+1}(kd) \end{Bmatrix} \zeta_2^{(2m+1)}$$

$$+ \begin{Bmatrix} H_{2n}^{(1)}(kd) \\ H_{2n}^{(1)\prime}(kd) \end{Bmatrix} \zeta_3^{(2n)} = \varepsilon_n \begin{Bmatrix} J_{2n}(kd) \\ J'_{2n}(kd) \end{Bmatrix} \zeta_0 , \tag{28}$$

where $n=0, 1, 2, \cdots$, the quantities in the wavy brackets being taken in the same order.

The above infinite simultaneous equations are final forms on which the approximation of the expressions of the buffer domain are given.

Before such approximation, modifications of the formal expressions described in *2,4* are performed by use of (26) and (27).

2,6. Simplifications of the Formal Expressions.

Let $\zeta_1^{(sc)}$ be a scattered wave in the domain D_1. The expression (8) becomes

$$\left.\begin{aligned} \zeta_1 &= 2\zeta_0 \cos ky + \zeta_1^{(sc)} , \\ \zeta_1^{(sc)} &= \sum_{m=0}^{\infty} \zeta_1^{(2m)} H_{2m}^{(1)}(kr) \cos 2m\theta . \end{aligned}\right\} \tag{29}$$

If one considers the waves at points symmetrical with the x-axis, i.e. (r, θ_1) and (r, θ_3) for $\theta_1 = -\theta_3$ $(0<\theta_1<\pi)$, the scattered waves $\zeta_1^{(sc)}$ in the domain D_1 are, using (27), expressed by those in the domain D_3 as follows.

$$\left.\begin{aligned} &\zeta_1^{(sc)}(r, \theta_1) \\ &= \zeta_1^{(sc)}(r, \theta_3) \\ &= -\zeta_3(r, \theta_3) , \end{aligned}\right\} \tag{30}$$

where the equality of the first two expressions are due to the symmetry of cosine function for the x-axis.

From the above result, it turns out that the scattered waves on

both sides of a straight breakwater behave asymmetrically in such a way that these waves at the points symmetrical with the breakwater are out of phase by π, and that the amounts of the amplitudes of the waves are equal to each other.

Since the unknowns $\zeta_1^{(2m)}$ have been excluded from the infinite simultaneous equations (28) in *2,5*, the formal expressions in the domains D_1 and D_3 are rewritten as follows.

$$\zeta_1(r\ ,\ \theta_1)=2\zeta_0\cos ky-\zeta_3(r\ ,\ \theta_3)\ , \tag{31}$$

$$\zeta_3(r\ ,\ \theta_3)=\sum_{m=0}^{\infty}\zeta_3^{(2m)}H_{2m}^{(1)}(kr)\cos 2m\theta_3\ , \tag{32}$$

where $\theta_1=-\theta_3$ for $0<\theta_1<\pi$.

Let us next consider the waves in the domain D_2.

A substitution of (26) into (10) yields

$$\zeta_2=\zeta_0\sum_{m=0}^{\infty}\varepsilon_m J_{2m}(kr)\cos 2m\theta+\sum_{m=0}^{\infty}\zeta_2^{(2m+1)}J_{2m+1}(kr)\sin(2m+1)\theta\ .$$

And taking account of the relation (16), the above expression is also reduced to

$$\zeta_2=\zeta_0\cos ky+\sum_{m=0}^{\infty}\zeta_2^{(2m+1)}J_{2m+1}(kr)\sin(2m+1)\theta\ . \tag{33}$$

This expression is a final form to be obtained in the domain D_2.

Here, attention is focussed on the behavior of the wave on the line running between either corner of the mouth of a breakwater.

Setting down

$$y=0 \text{ or } \theta=0 \text{ for } 0<x<d \text{ and } \pi \text{ for } 0>x>-d$$

in (33), (33) becomes

$$\zeta_2=\zeta_0\ .$$

This expression denotes that the amplitude of the wave on the straight line mentioned above are rigidly equal to that of the incident wave for *any* value of kd.

2,7. The Zeroth Approximation.

In this section, a limiting case

$$kd\simeq 0$$

is considered. This case denotes that the invading waves are very long in wave-length as compared with the breadth of the mouth of a breakwater.

Then the approximations

$$\left.\begin{aligned} &J_0(kr)\neq 0 \\ &J_m(kr)=0 \quad (m\geqq 1) \end{aligned}\right\} \quad \text{for } r\leqq d \tag{34}$$

are admissible.

Using (34), the infinite simultaneous equations (28) become

$$\begin{Bmatrix} H_0^{(1)}(kd) \\ H_0^{(1)\prime}(kd) \end{Bmatrix} \zeta_3^{(0)} = \begin{Bmatrix} J_0(kd) \\ J_0'(kd) \end{Bmatrix} \zeta_0 \tag{35}$$

and

$$i\cdot \begin{Bmatrix} Y_{2n}(kd) \\ Y_{2n}'(kd) \end{Bmatrix} \zeta_3^{(2n)} = 0 \quad (n\geqq 1)\,. \tag{36}$$

From (35), when $kd\simeq 0$,

$$\zeta_3^{(0)}=0$$

because of $Y_0(kd)\to-\infty$ $(kd\to 0)$.

From (36),

$$\zeta_3^{(2n)}=0$$

for $n\geqq 1$.

Substituting the above two expressions into (32), it is found that the waves in the domain D_3 vanish when $kd\to 0$, i.e.

$$\zeta_3(r\,,\,\theta_3)=0\,. \tag{37}$$

Then the expression

$$\zeta_1(r\,,\,\theta_1)=2\zeta_0\cos ky \tag{38}$$

follows from (31).

The last equation stands for an occurrence of complete standing waves in the domain D_1 without any disturbance due to the mouth of a breakwater.

Putting the approximation (34) into (33), the expression of the waves in the domain D_2 becomes

$$\zeta_2=\zeta_0\cos ky\,. \tag{39}$$

This expression says that the waves in the mouth of a breakwater behave like standing waves with the same amplitude as that of the incident waves. But since our consideration is made under the condition $kd\simeq 0$, it seems to terminate in estimating the rough behavior of the waves.

At any rate, when kd is very small, a gradient of the wave height around the mouth of a breakwater is, from (37)-(39), very large. When a theory is developed on the basis of a long wave equation, a velocity of water particles is proportional to a gradient of the water surface. Therefore, the velocities of water particles begin to be so great in this region that the use of a long wave equation might be doubtful for the sake of predominance of inertia terms in the equation of motion, which are neglected in a long wave equation used in the present work.

For the reasons mentioned above, no further computations and discussions are performed.

2,8. The (2l+1) th Approximation.

In this section, a theory of the $(2l+1)$ th approximation ($l=0, 1, 2,$ - - -) is presented.

In order to make the infinite simultaneous equations (28) approachable to actual calculations, the approximation is bestowed on the expressions of the buffer domain or the domain D_2.

The meaning of the $(2l+1)$ th approximation is as follows:—

In the expression of the buffer domain, the Bessel functions $J_m(kr)$ for $r\leqq d$ are retained up to $m=2l+1$ (l: non-negative integers) and those above $m=2l+1$ are neglected, i.e.,

$$\begin{aligned} J_m(kr)&\neq 0 \qquad (m\leqq 2l+1)\\ J_m(kr)&=0 \qquad (m>2l+1)\end{aligned} \tag{40}$$

for $r\leqq d$, where $l=0, 1, 2,$- - -.

The formal expression in the buffer domain D_2 then becomes, from (33),

$$\zeta_2=\zeta_0\cos ky+\sum_{m=0}^{l}\zeta_2^{(2m+1)}J_{2m+1}(kr)\sin(2m+1)\theta\,. \tag{41}$$

Applying the approximation (40) to (28), these equations are reduced to the following:—

$$\frac{2}{\pi}\varepsilon_n\sum_{m=0}^{l}\frac{(2m+1)}{(2m+1)^2-(2n)^2}\begin{Bmatrix}J_{2m+1}(kd)\\ J'_{2m+1}(kd)\end{Bmatrix}\zeta_2^{(2m+1)}$$

$$+\begin{Bmatrix}H_{2n}^{(1)}(kd)\\ H_{2n}^{(1)\prime}(kd)\end{Bmatrix}\zeta_3^{(2n)}=\varepsilon_n\begin{Bmatrix}J_{2n}(kd)\\ J'_{2n}(kd)\end{Bmatrix}\zeta_0 \tag{42}$$

for $n=0, 1, 2,---l$,
and

$$\frac{2}{\pi}\varepsilon_n\sum_{m=0}^{l}\frac{(2m+1)}{(2m+1)^2-(2n)^2}J_{2m+1}(kd)\zeta_2^{(2m+1)}+iY_{2n}(kd)\zeta_3^{(2n)}=0 \tag{43}$$

for $n=l+1,\ l+2,\ ---$,
where l is a non-negative integer referring to the $(2l+1)$ th approximation and where the quantities in the wavy brackets of (42) must be taken in the same order.

Now, if one specifies the value of l or the degree of the approximation, the unknowns

$$\zeta_2^{(2n+1)} \text{ and } \zeta_3^{(2n)} \quad (n=0\,,\ 1\,,\ 2\,,---\,,\ l)$$

are readily calculated from the simultaneous equations (42), the higher modes

$$\zeta_3^{(2n)} \quad (n=l+1\,,\ l+2\,,---)$$

being obtained by a substitution of $\zeta_2^{(2n+1)}$ $(n=0\,,\ 1\,,\ 2,---\,,\ l)$ into (43).

Using the unknown factors obtained in such a way, the behaviors of the waves in the vicinity of the mouth of a breakwater are elucidated numerically through formal expressions (31), (32) and (41).

The actual calculations of the above-mentioned procedures are carried out with the aid of an electronic computer.

In the following sections, numerical calculations and discussions of the results are made.

3. Numerical Calculations and Discussions

In the present work, endeavour is devoted primarily to a development of a theory with only a few numerical calculations made.

3,1. Check of Convergence

In this paragraph, a check of convergence is carried out through

the calculations of the amplitude in six directions, i.e., $\theta=0+\varepsilon$, $\pi/4$, $\pi/2$, and $0-\varepsilon$, $-\pi/4$, $-\pi/2$ (ε is an infinitesimal) for parameters $kd=0.1$, 0.5, 1.0, 1.5 and 2.0. These curves are sketched in Figs. 3 to 32. According to these figures, convergences of the theories under the cited approximations in each figure are fairly good except for the nearby part of $r/d=1.0$ (the neighbouring region of the domains D_2 and D_1 (or D_3)) in which a little disagreement of the approximated curves is seen. Such disagreement is ascribed to a deficiency of the adopted approximations. In the formal expressions (8) to (10), the higher modes contribute significantly to these expressions in the nearby part of $r/d=1.0$, such contributions decaying rapidly when departing from $r/d=1.0$. As seen in the variations along the breakwater (Figs. 3, 6, 9, 12, 15, 18, 21, 24, 27 and 30), the amplitudes around points ($x=\pm d$, $y=0$) are not always smooth. The singularity of the corner points of the breakwater might be considered to cause the disagreement of the approximated curves. In order to avoid such disagreement, we must calculate the theory under a more generalized approximation, but, in our formulation of the theory, the computation has arrived at a state of overflow in an electronic computer which is due to an existence of $Y_m(x)$ (the second kind of the Bessel function) and the number of the element of the simultaneous equations. A further consideration is, therefore, required to bury the lack of agreement in formulation of the approximated theory.

3,2. Variations of Amplitude in Typical Directions

Referring to Figs. 3 to 32, the variation of the amplitude along these directions is discussed. These figures (Figs. 3 to 32) are depicted in large scale for convenience of experiment.

In Figs. 3, 9, 15, 21, and 27 (the curves of the amplitude along the forward part of the wall of a breakwater), an outstanding feature is an appearance of undulatory variation of the amplitude having $|\zeta|=2.0$ as the axis of the undulation. Among them all, the first undulation has the largest amplitude, the subsequent ones beginning to be small in amplitude leaving from the mouth of a breakwater. Such undulation is caused by rotating waves occurring in the forward sea of a breakwater, as will be seen later in the figure showing the overall variation of phase of the waves. A similar phenomenon was found in the works[13] concerning a long wave in the vicinity of an estuary, in which, though rotating waves were not ascertained definitely, diverted waves appear

13) T. Momoi, *Bull. Earthq. Res. Inst.*, **44** (1966), 1009-1040.

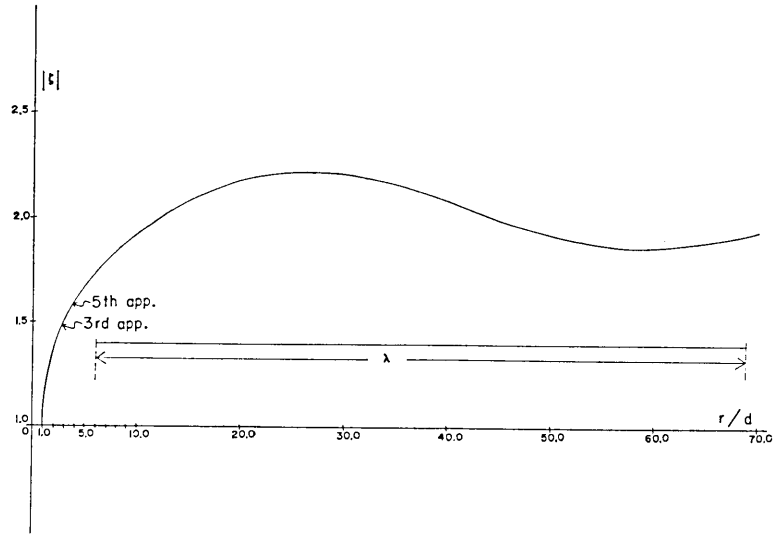

Fig. 3. Variation of amplitude $|\zeta|$ along the forward wall of a breakwater ($\theta=0+\varepsilon$) for $kd=0.1$.

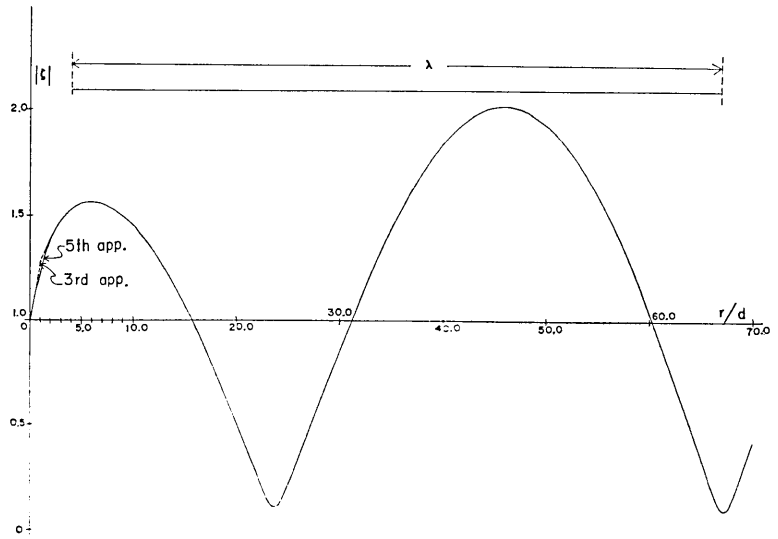

Fig. 4. Variation of amplitude $|\zeta|$ along the direction $\theta=\pi/4$ in the forward waters of a breakwater for $kd=0.1$.

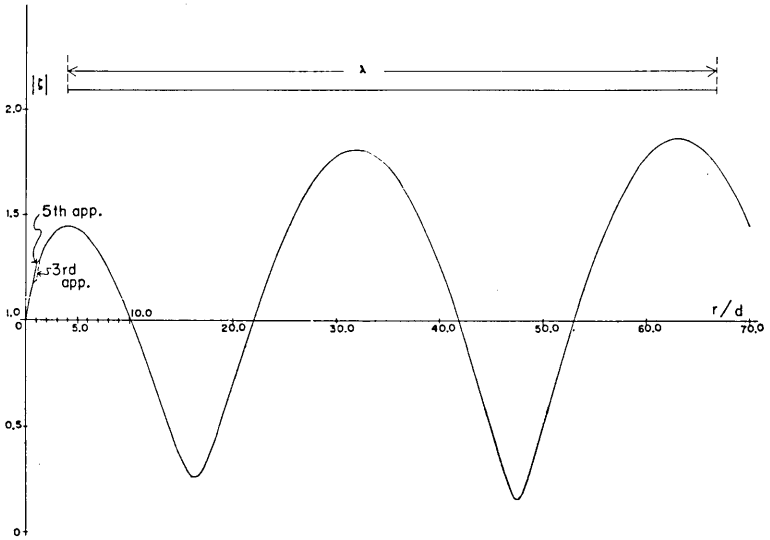

Fig. 5. Variation of amplitude $|\zeta|$ along the direction $\theta=\pi/2$ in the forward waters of a breakwater for a specified value of $kd=0.1$.

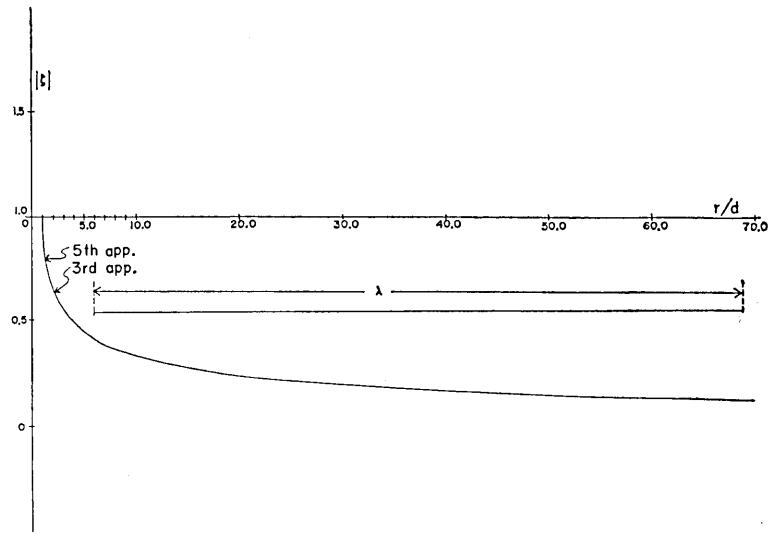

Fig. 6. Variation of amplitude $|\zeta|$ along the wall $(\theta=0-\varepsilon)$ in the rear waters of a breakwater for $kd=0.1$.

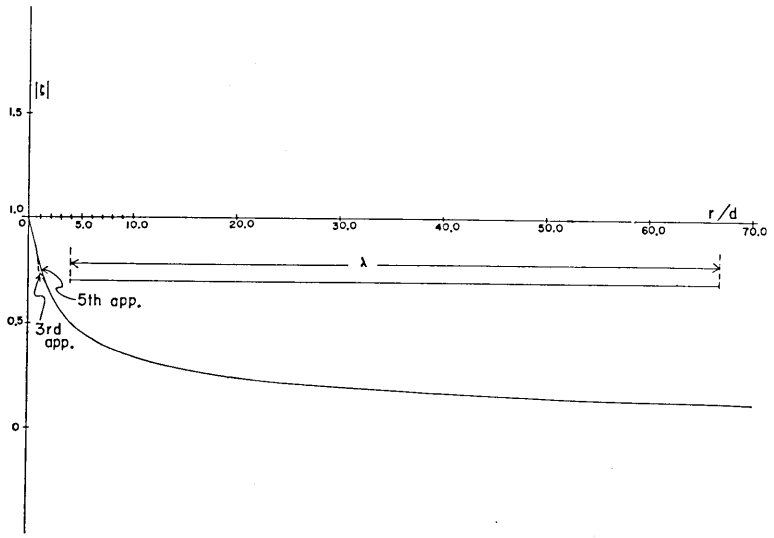

Fig. 7. Variation of amplitude $|\zeta|$ along the direction $\theta=-\pi/4$ in the backward waters of a breakwater for a specified value $kd=0.1$.

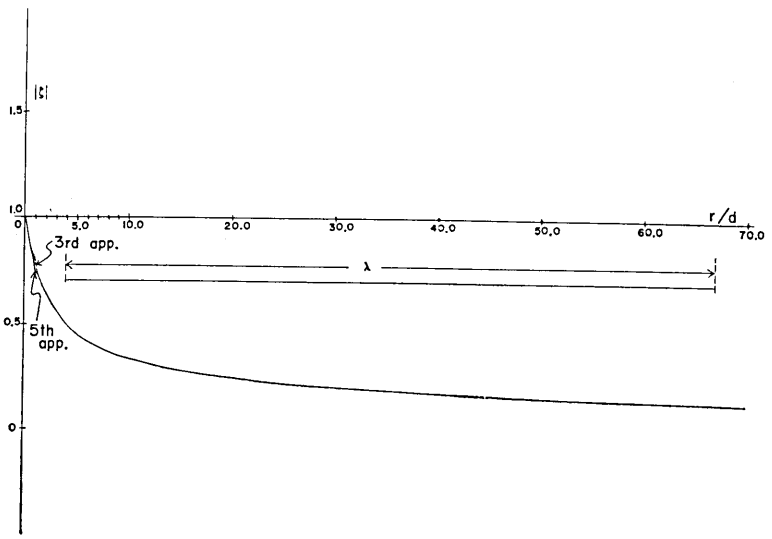

Fig. 8. Variation of amplitude $|\zeta|$ along the direction $\theta=-\pi/2$ in the backward waters of a breakwater for a specified value $kd=0.1$.

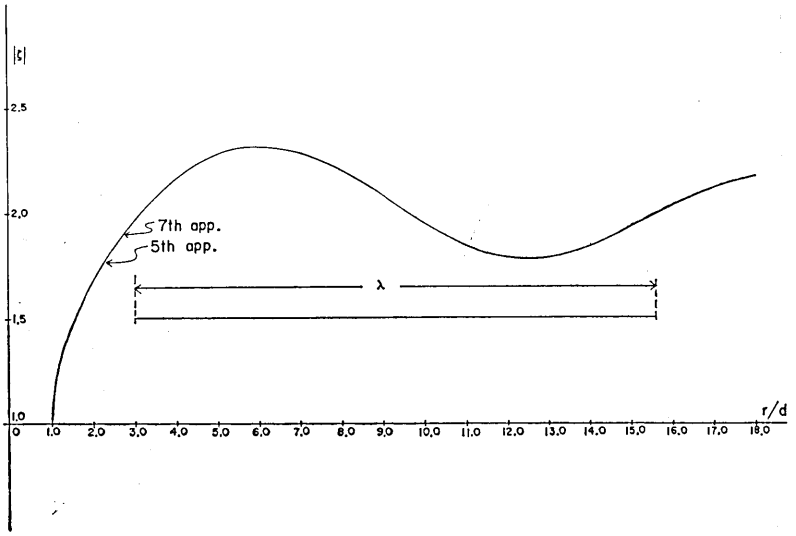

Fig. 9. Variation of amplitude $|\zeta|$ along the forward wall of a breakwater ($\theta=0+\varepsilon$) for a specified value $kd=0.5$.

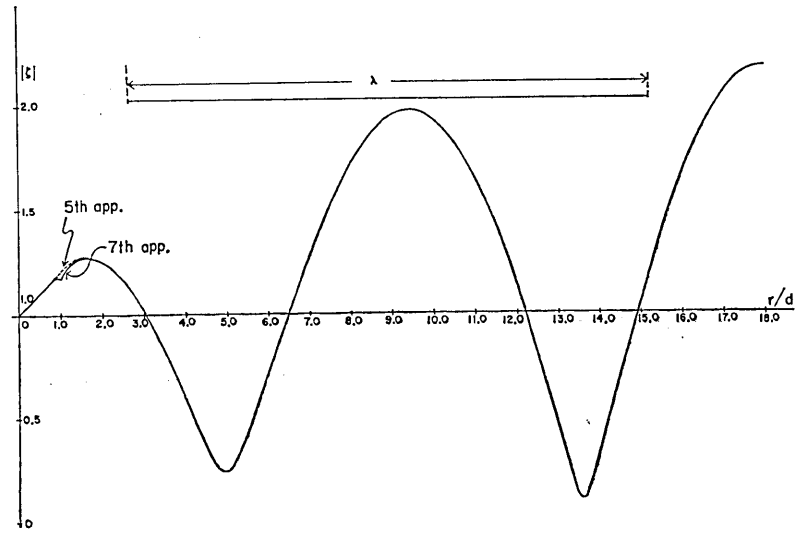

Fig. 10. Variation of amplitude $|\zeta|$ along the direction $\theta=\pi/4$ in the forward sea of a breakwater for $kd=0.5$.

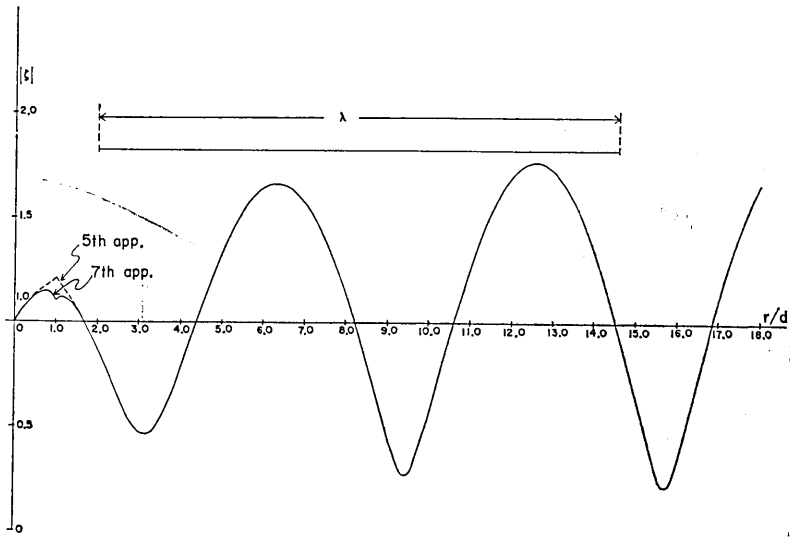

Fig. 11. Variation of amplitude $|\zeta|$ along the direction $\theta=\pi/2$ in the forward waters of a breakwater for $kd=0.5$.

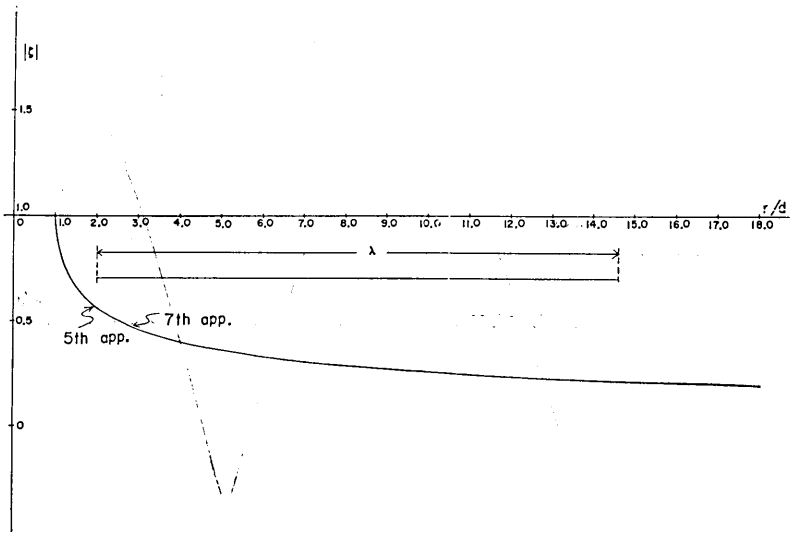

Fig. 12. Variation of amplitude $|\zeta|$ along the wall $(\theta=0-\varepsilon)$ in the backward waters of a breakwater for $kd=0.5$.

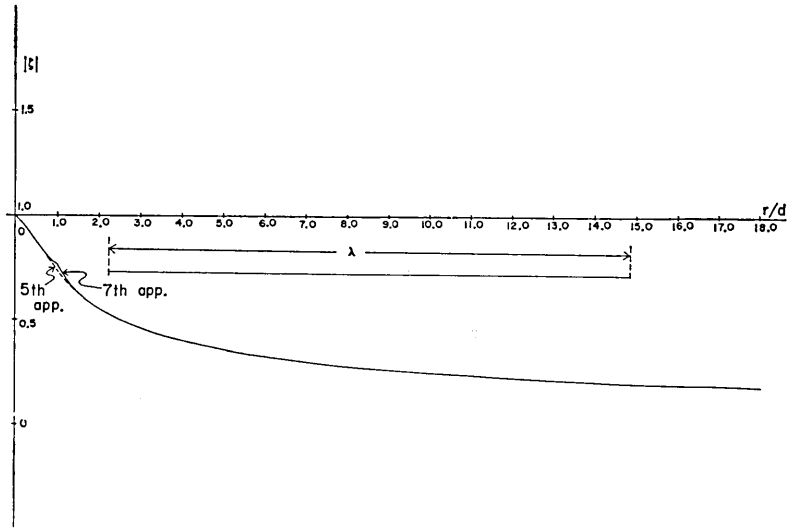

Fig. 13. Variation of amplitude $|\zeta|$ along the direction $\theta=-\pi/4$ in the backward waters for a specified value $kd=0.5$.

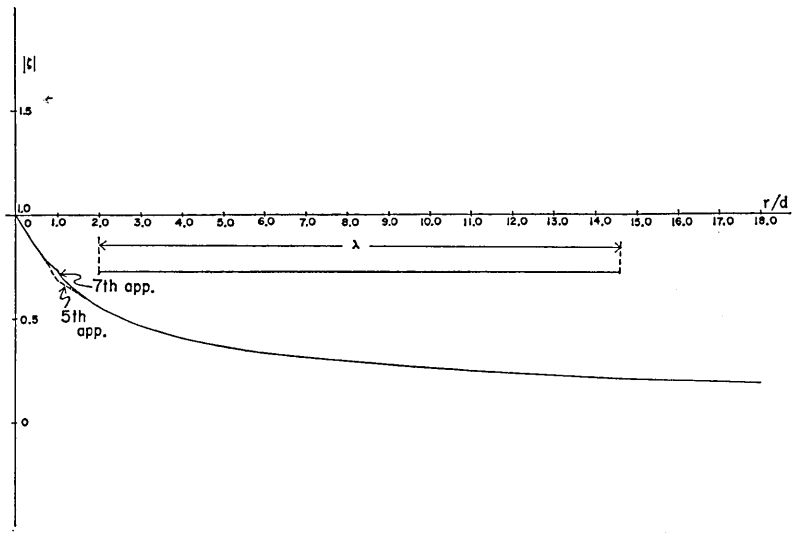

Fig. 14. Variation of amplitude $|\zeta|$ along the direction $\theta=-\pi/2$ in the rear waters of a breakwater for $kd=0.5$.

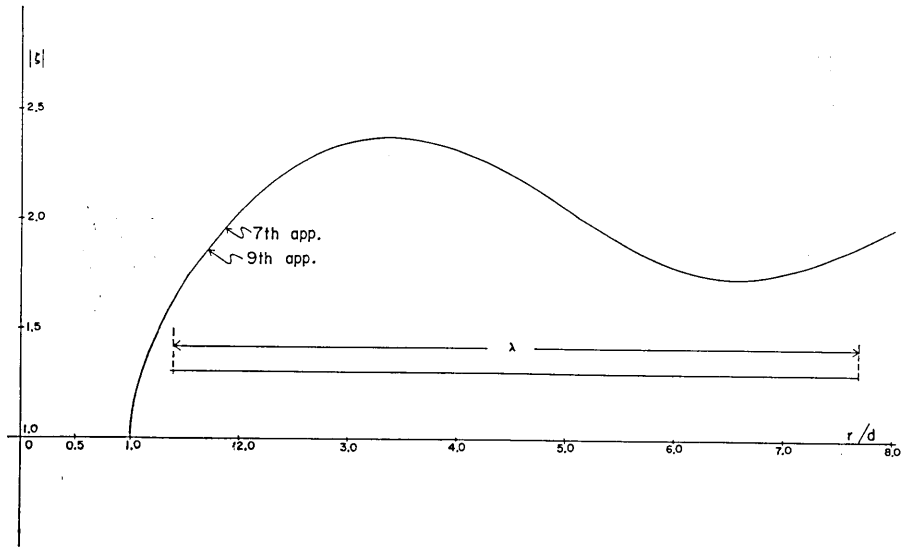

Fig. 15. Variation of amplitude $|\zeta|$ along the forward wall of a breakwater ($\theta=0+\varepsilon$) for a specified value $kd=1.0$.

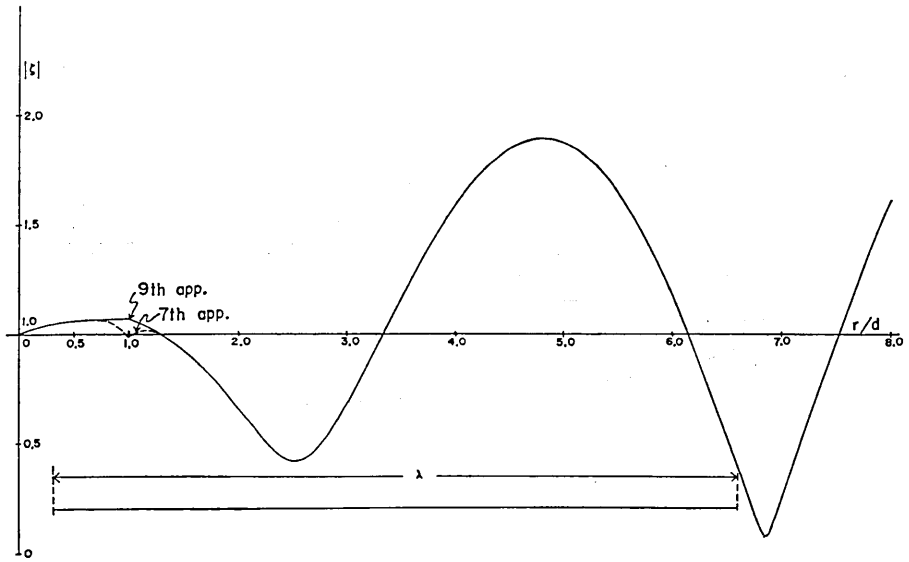

Fig. 16. Variation of amplitude $|\zeta|$ along the direction $\theta=\pi/4$ in the forward sea of a breakwater for $kd=1.0$.

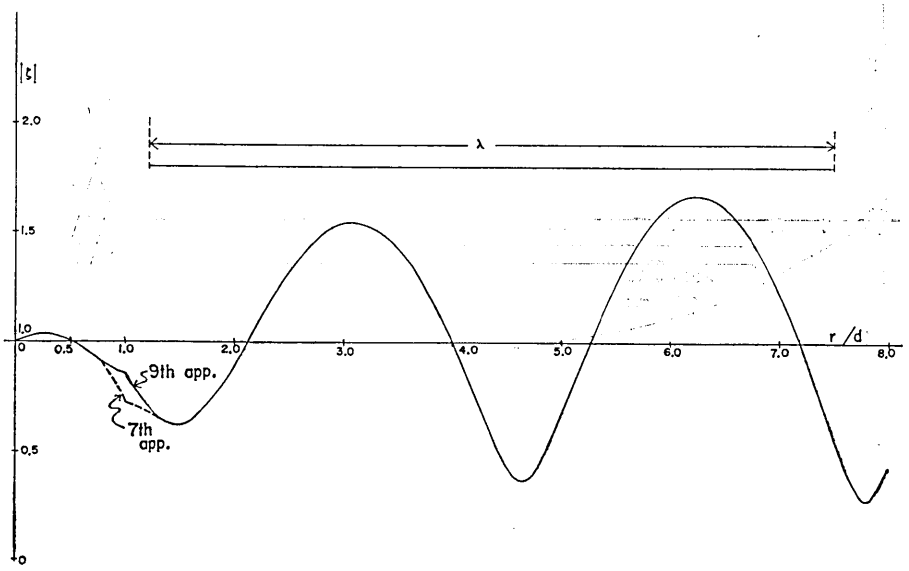

Fig. 17. Variation of amplitude $|\zeta|$ along the direction $\theta=\pi/2$ in the forward sea of a breakwater for a parameter $kd=1.0$.

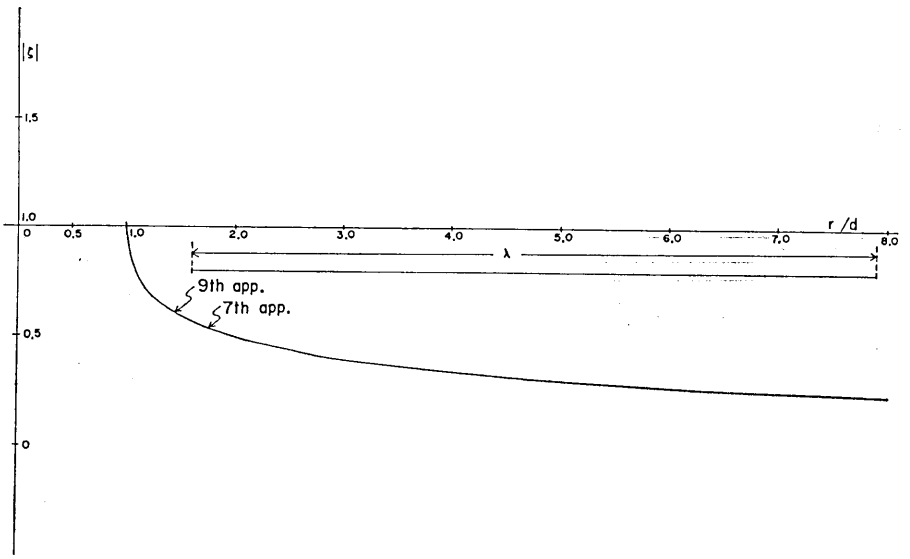

Fig. 18. Variation of amplitude $|\zeta|$ along the rear side of the wall ($\theta=0-\varepsilon$) of a breakwater for $kd=1.0$.

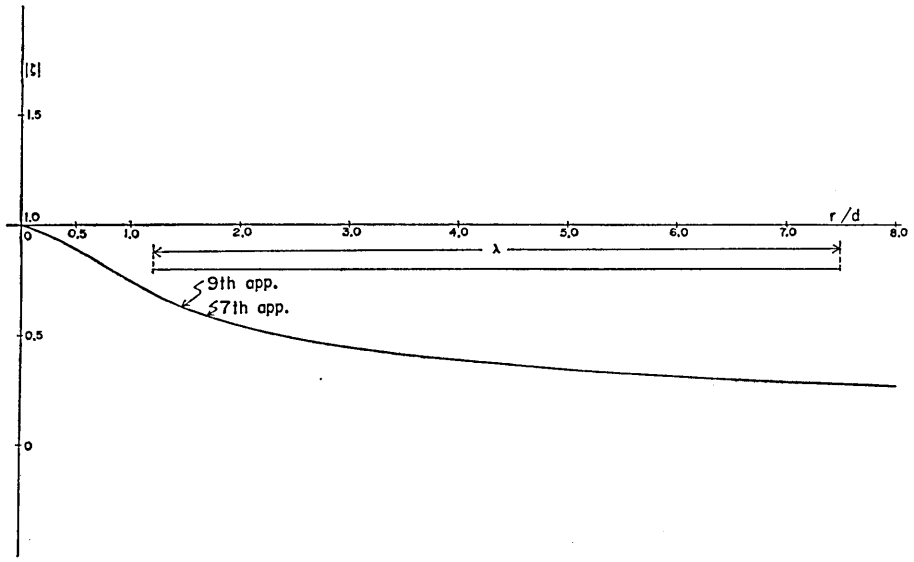

Fig. 19. Variation of amplitude $|\zeta|$ along the direction $\theta=-\pi/4$ in the backward waters of a breakwater for $kd=1.0$.

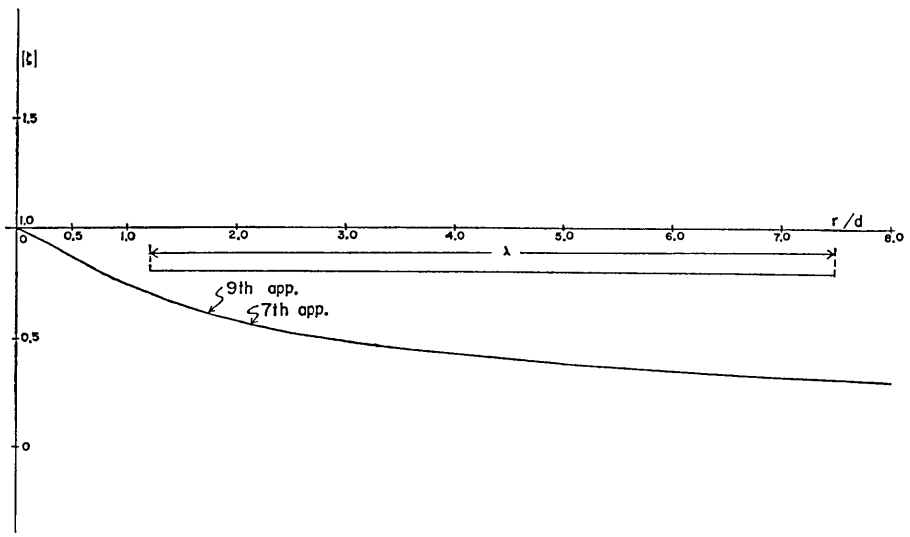

Fig. 20. Variation of amplitude $|\zeta|$ along the direction $\theta=-\pi/2$ in the rear waters of a breakwater for a parameter $kd=1.0$.

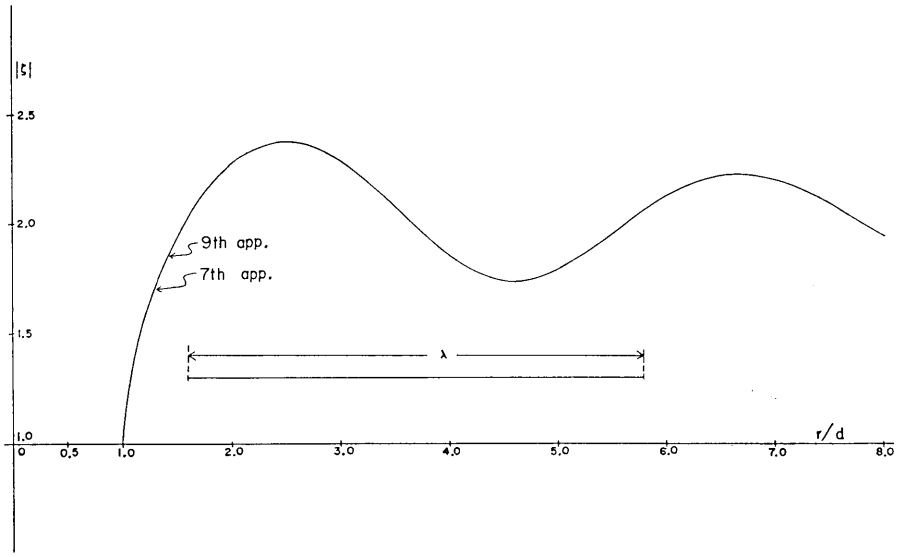

Fig. 21. Variation of amplitude $|\zeta|$ along the forward wall of a breakwater ($\theta=0+\varepsilon$) for a specified parameter $kd=1.5$.

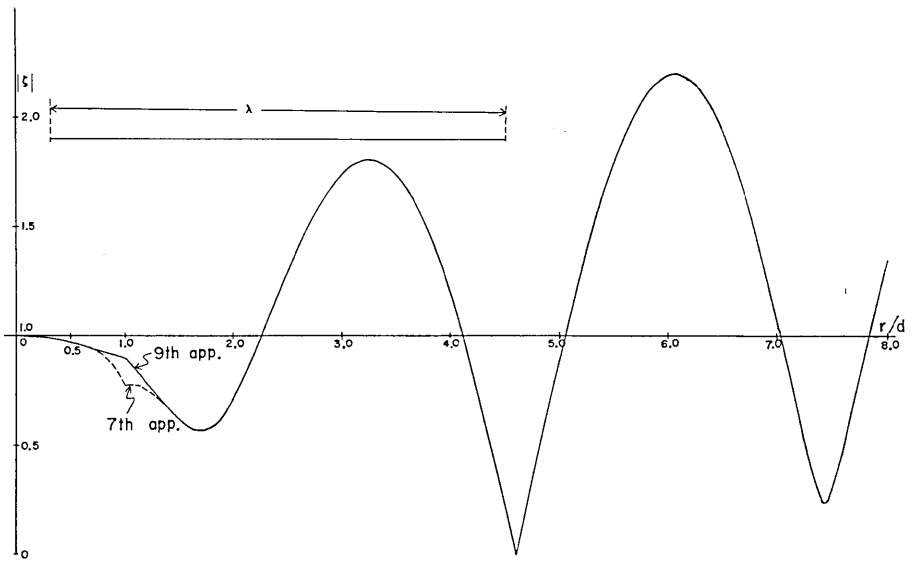

Fig. 22. Variation of amplitude $|\zeta|$ along the direction $\theta=\pi/4$ in the forward waters of a breakwater for $kd=1.5$.

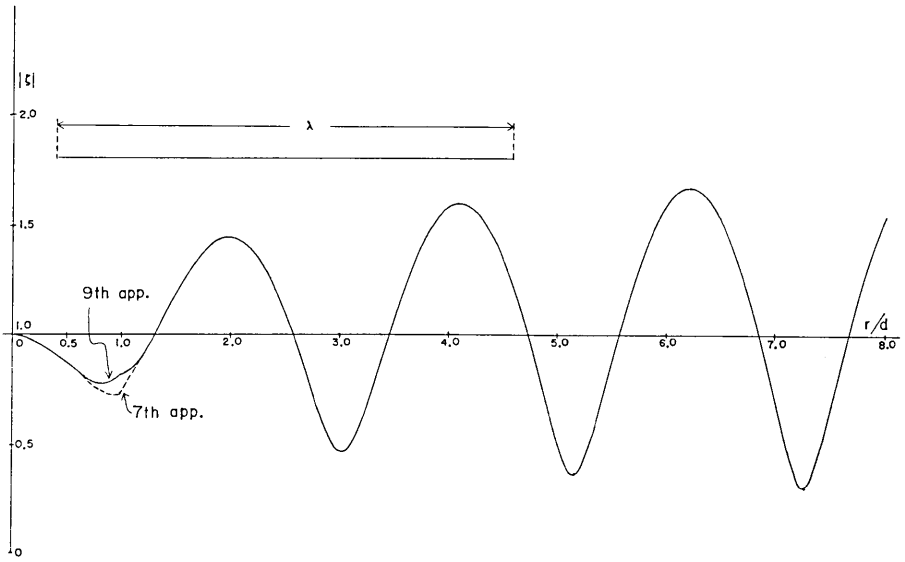

Fig. 23. Variation of amplitude $|\zeta|$ along the direction $\theta=\pi/2$ in the forward sea of a breakwater for $kd=1.5$.

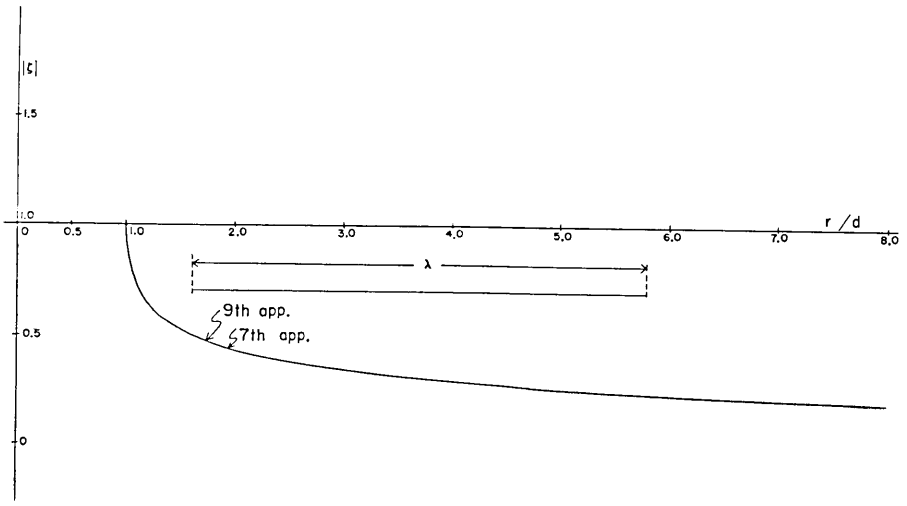

Fig. 24. Variation of amplitude $|\zeta|$ along the rear side of the wall of a breakwater ($\theta=0-\varepsilon$) for a parameter $kd=1.5$.

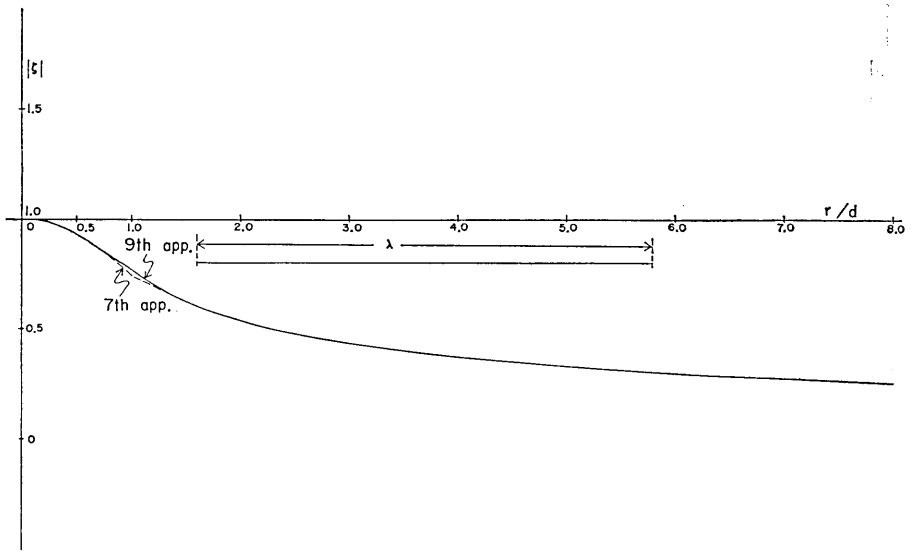

Fig. 25. Variation of amplitude $|\zeta|$ along the direction $\theta=-\pi/4$ in the backward waters of a breakwater for a specified parameter $kd=1.5$.

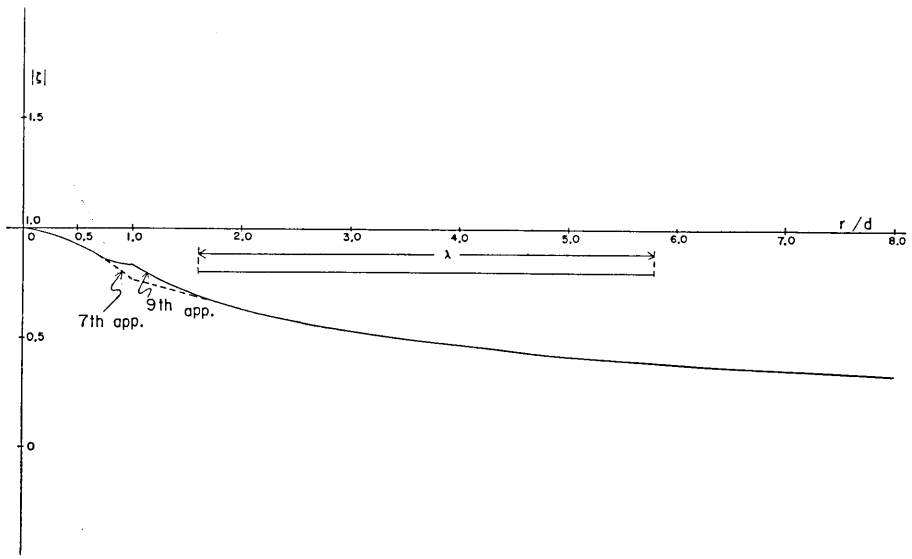

Fig. 26. Variation of amplitude $|\zeta|$ along the direction $\theta=-\pi/2$ in the backward waters of a breakwater for a parameter $kd=1.5$.

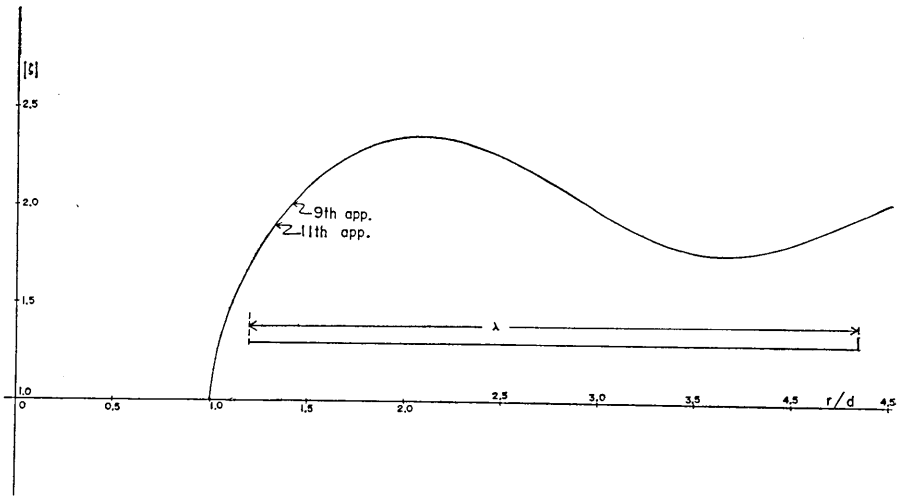

Fig. 27. Variation of amplitude $|\zeta|$ along the foward wall of a breakwater ($\theta=0+\varepsilon$) for a specified value of $kd=2.0$.

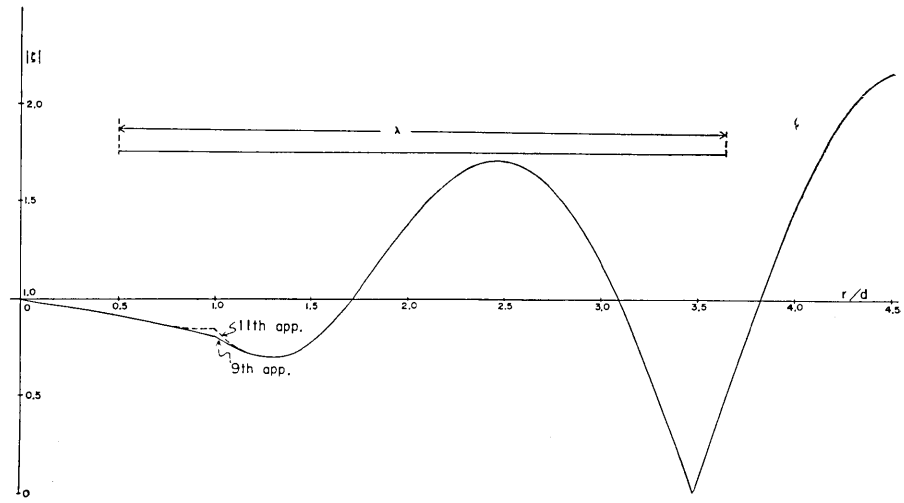

Fig. 28. Variation of amplitude $|\zeta|$ along the direction $\theta=\pi/4$ in the forward waters of a breakwater for $kd=2.0$.

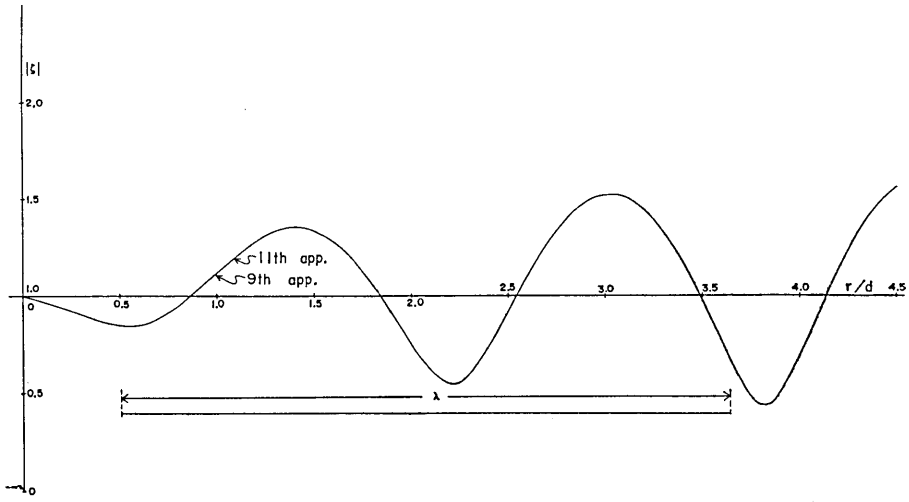

Fig 29. Variation of amplitude $|\zeta|$ along the direction $\theta=\pi/2$ in the forward sea of a breakwater for $kd=2.0$.

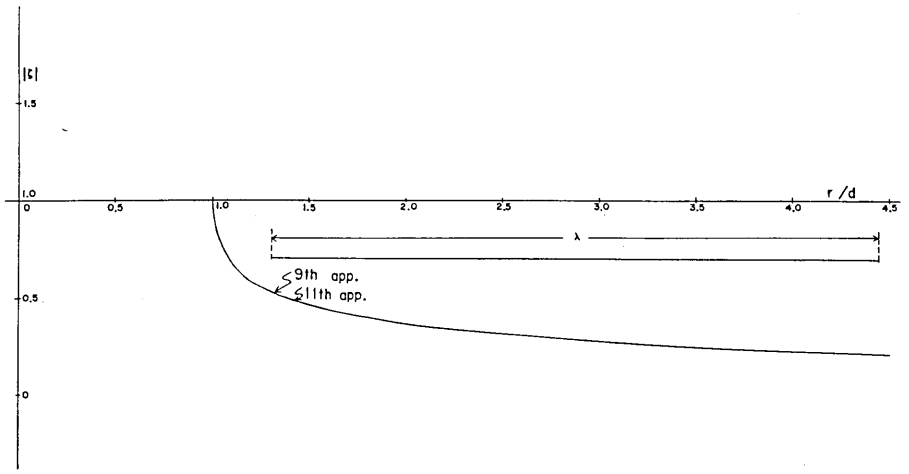

Fig. 30. Variation of amplitude $|\zeta|$ along the rear side of the wall of a breakwater ($\theta=0-\varepsilon$) for a parameter $kd=2.0$.

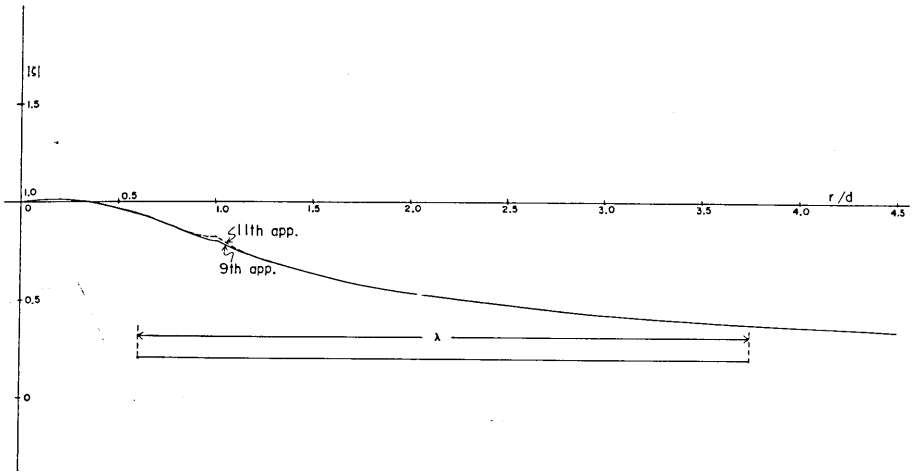

Fig. 31. Variation of amplitude $|\zeta|$ along the direction $\theta=-\pi/4$ in the backward sea of a breakwater for a specified parameter $kd=2.0$.

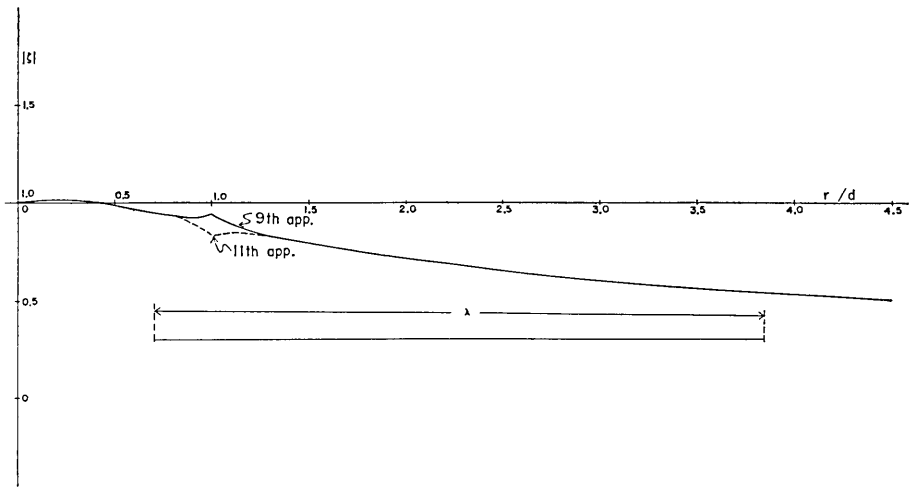

Fig. 32. Variation of amplitude $|\zeta|$ along the direction $\theta=-\pi/2$ in the backward sea of a breakwater for a parameter $kd=2.0$.

in the nearby part of an estuary causing high waves at the straight coast. Through Figs. 3 to 32, a scale of a wave-length (λ) of the incident waves has been drawn in. Comparing this wave-length and a change of the amplitude in the figures, it turns out that the undulation of the amplitude along the forward wall of a breakwater is repeated with nearly a wave-length of the incident waves.

Noticing the variations of the amplitude in the direction of the incident waves (perpendicular to a breakwater) (Figs. 5, 11, 17, 23 and 29), the amplitude undulates nearly every half a wave-length of the incident waves. The amplitude of these undulations is increased gradually as r increases, which might be considered to tend eventually to a unit.

In the figures showing the amplitudes in the direction $\theta=\pi/4$, the undulatory variations have approximately a wave-length of two-thirds of that of the invading waves (refer to Figs. 4, 10, 16, 22 and 28).

For the reader's convenience, the wave-lengths of the undulatory motions of the amplitude in three directions, i.e., $\theta=0+\varepsilon$, $\pi/4$ and $\pi/2$ are sketched in Fig. 33.

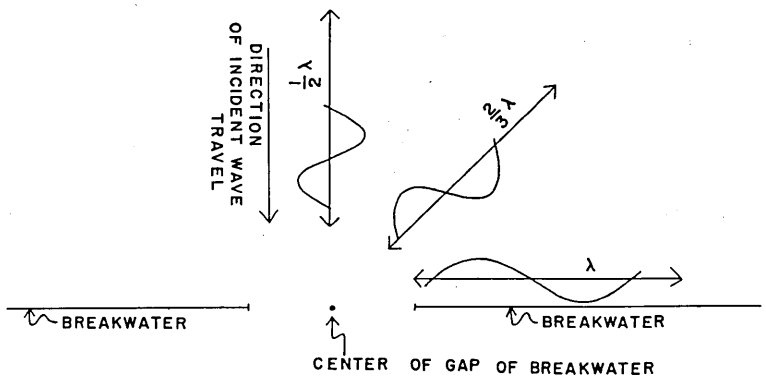

Fig. 33. Figurative explanation of a wave-length of the undulatory variations of amplitude in three typical directions in the forward sea (λ: a wave-length of the incident waves).

In the above figures (Figs. 4, 10, 22 and 28) except for Fig. 16, it is found that the top of the second or third undulation exceeds in height twice the amplitude of the incident waves. Such extraordinary high waves are a counterpart of the high waves occurring at shore, both of which are produced by rotating or reflected waves near the mouth of a breakwater (This reasoning is ascertained later by the figures showing

the overall variations of the amplitude and phase near the mouth of a breakwater).

As far as the variations of the amplitude in the backward sea of a breakwater are concerned, the amplitudes are in general decreased as r increases (see Figs. 6, 7, 8, 12, 13, 14, 18, 19, 20, 24, 25, 26, 30, 31, 32). The primary part of the decrease takes place in the nearby region of the mouth of a breakwater.

Table 1. The values of $|\zeta|$ at $r=\lambda+d$ in the backward sea of a breakwater*)

θ \ kd	0.1	0.5	1.0	1.5	2.0
$0-\varepsilon$	0.138	0.216	0.253	0.252	0.230
$-\pi/4$	0.139	0.219	0.287	0.331	0.357
$-\pi/2$	0.140	0.230	0.319	0.417	0.519

Inspection of Table 1 reveals that the rate of decrease of the amplitude (the decrement of the amplitude for a distance λ) is greater for small kd (=0.1 to 1.0) than for large kd (=1.0 to 2.0). Since the amplitude of the waves on the line connecting two corners of a breakwater, as shown in Section *2,6. (Simplifications of the Formal Expressions)*, is a unit (equal to the amplitude of the incident waves), the wave heights for parameters $kd=0.1$, 0.5, 1.0, 1.5 and 2.0 are decayed from a unit to about 0.139, 0.219, 0.287, 0.331 and 0.357 respectively as r increases from 0 to $\lambda+d$ in the rear side of a breakwater.

In Table 1, another feature is found such that large wave-length of the invading waves (corresponding to small kd) favors the diffraction of the waves in the rear waters of a breakwater.**) When $kd=0.1$, no directivity is seen for the waves transmitted through the mouth of a breakwater. As kd is increasing, the amplitude in the direction of $\theta=-\pi/2$ begins to be large gradually as compared with that in the direction $\theta=0-\varepsilon$. When kd becomes 2.0, the amplitude of the former amounts to nearly twice that of the latter. Such tendency of directivity (convergence of the energy along the direction of the incident wave) presumably grows severe with an increase of kd.

*) $r=\lambda+d$ is a point apart from the outer margin ($r=d$) of the buffer domain D_2 by a distance λ.

**) Such tendency is also found in the experiment made by *Mogi* (refer to the paper cited in the introduction), although his experiment was carried out for relatively large kd.

3,3. Overall Variations of Amplitude and Phase

In this paragraph, the behaviors of the waves in the nearby part of the mouth of a breakwater are elucidated for two specified parameters $kd=0.1$ and 1.0. The variations of the amplitude and phase for $kd=0.1$ are presented in Figs. 34 to 37, and those for $kd=1.0$ are shown in Figs. 38 to 41.

In Figs. 34 and 38 showing the variations of the amplitude in the forward sea of a breakwater for $kd=0.1$ and 1.0 respectively, a conspicuous feature is an appearance of high waves exceeding in height twice the amplitude of the incident waves. The feature is illustrated in Fig. 42, in which the regions of high waves are represented by "HIGH I" and "HIGH II". In Figs. 34 and 38, high waves are seen in only two parts, but such portion of high waves might extend to the outer region of the depicted figures, as supposedly shown in Fig. 42 (designated by "HIGH III", "HIGH I′" and "HIGH II′" and so on). Comparing two high waves in Fig. 34 or 38, the waves adjacent to the mouth of a breakwater (corresponding to "HIGH I" in Fig. 42) have a higher wave height than the high waves a little apart from the entrance of a breakwater (corresponding to "HIGH II" in Fig. 42). Among high waves hypothetically shown in Fig. 42, the part of "HIGH I" might have the highest wave height, and, leaving from the mouth of a breakwater, the wave height in the regions of the heigh waves presumably decreases gradually. Such a tendency is also conjectured from the figures showing the variations of the amplitude along the forward wall of a breakwater (Figs. 3, 9, 15, 21 and 27).

In Table 2, the values of a maximum wave height of the high waves in the forward sea (referred to "HIGH I" in Fig. 42) are tabulated for a change of kd. This table reveals that a maximum wave height along the forward wall of a breakwater increases with augmentation of kd from 0.1 to 1.5 and thereafter decreases to take a maximum at $kd=1.5$.

Comparing two figures relevant to the amplitude variation in the

Table 2. Maximum wave heights in the nearest part from the mouth of a breakwater

kd	0.1	0.5	1.0	1.5	2.0
$\|\zeta\|$	2.21	2.32	2.37	2.374 (maximum)	2.35

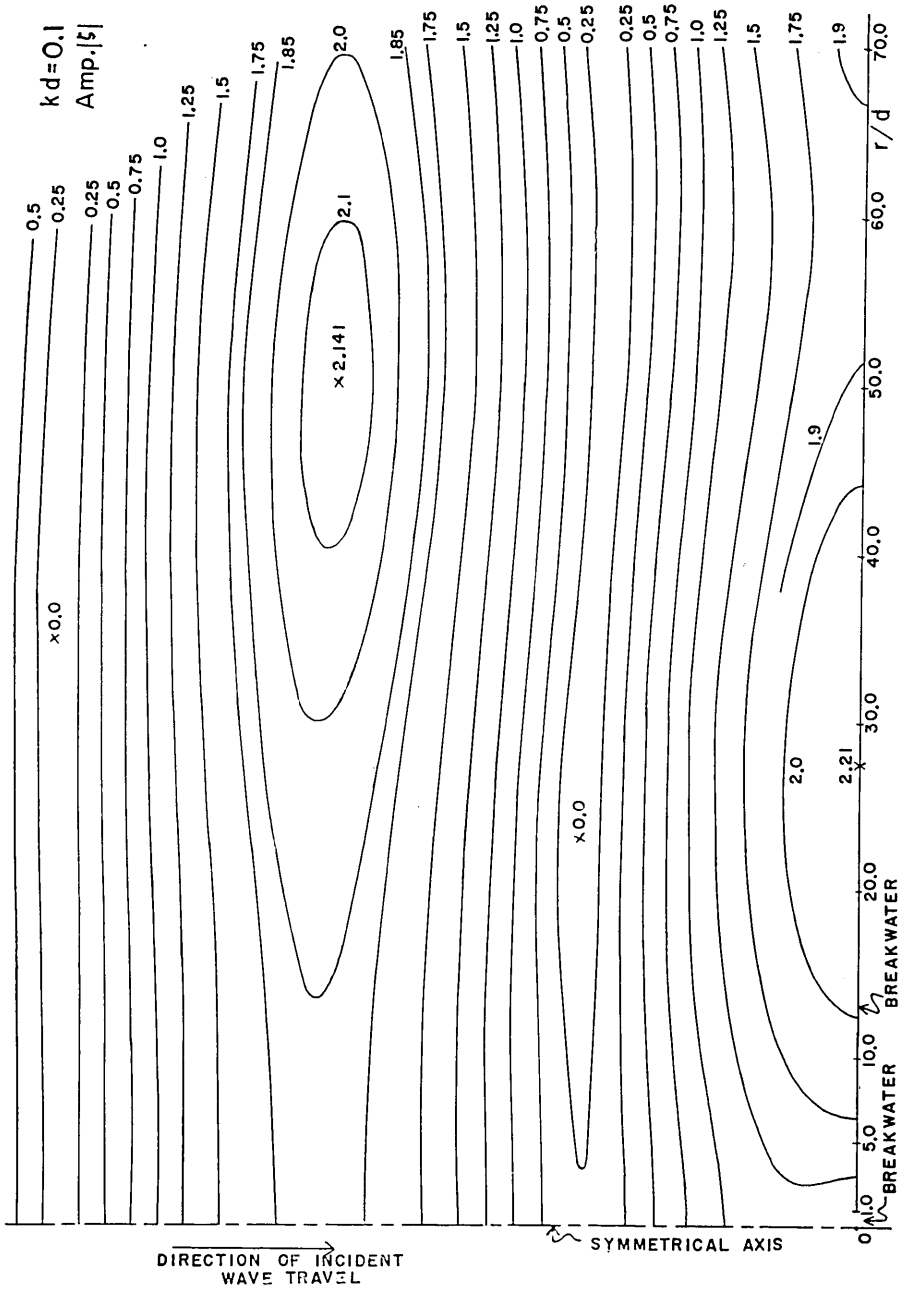

Fig. 34. Overall variation of amplitude $|\zeta|$ in the forward sea of a breakwater for a specified value $kd=0.1$. (The stated values in the figure denote those of $|\zeta|$ normalized by the amplitude of the incident waves ($=1.0$). Since the variation is symmetric for the straight line perpendicular to a breakwater passing through the center of a breakwater gap, only the right-hand figure is retained. The above figure is based on the theory of the 5th approximation.)

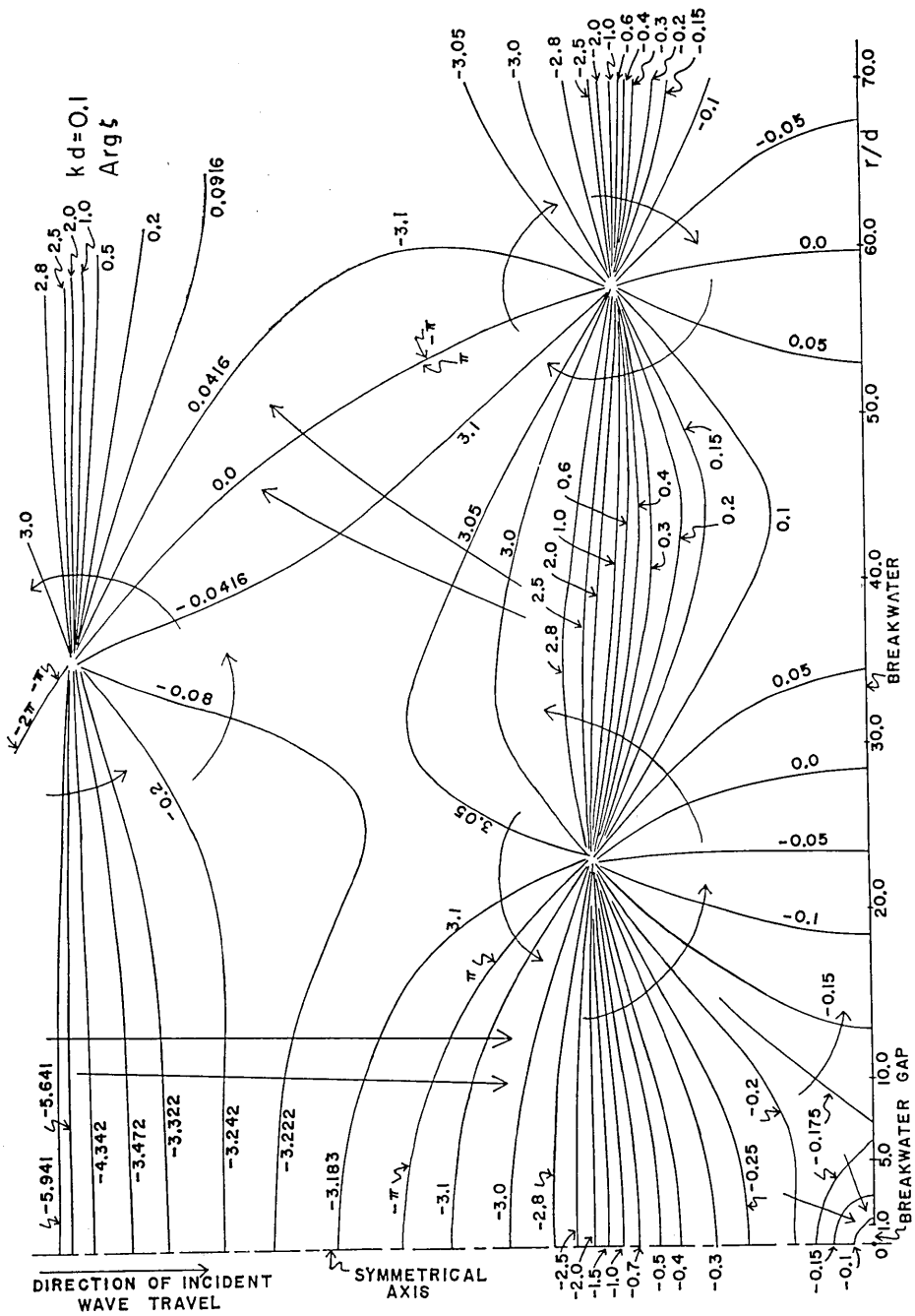

Fig. 35. Overall variation of phase arg ζ in the forward sea of a breakwater for a specified value $kd=0.1$. (The stated values in the figure denote arg ζ. Since the variation is symmetric for the straight line perpendicular to a breakwater wing passing through the center of a breakwater gap, only the right-hand figure is depicted. The above figure is based on the theory of the 5th approximation.)

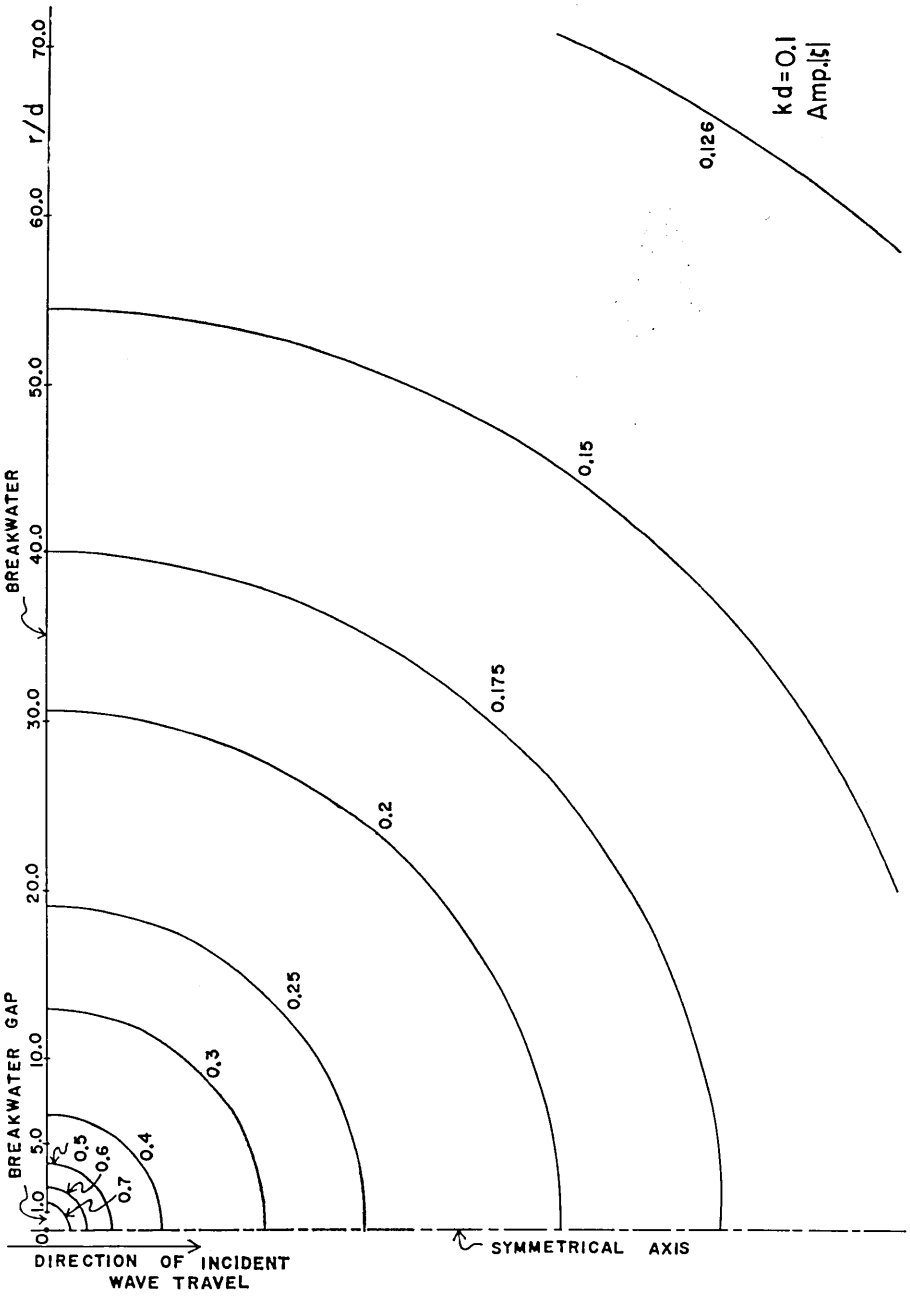

Fig. 36. Overall variation of amplitude $|\zeta|$ in the backward sea of a breakwater for a specified value $kd=0.1$. (The stated values in the figure denote amplitude $|\zeta|$ normalized by the amplitude of the incident waves. Only the right-hand variation is depicted owing to the symmetry of the phenomenon. The above figure is based on the theory of the 5th approximation.)

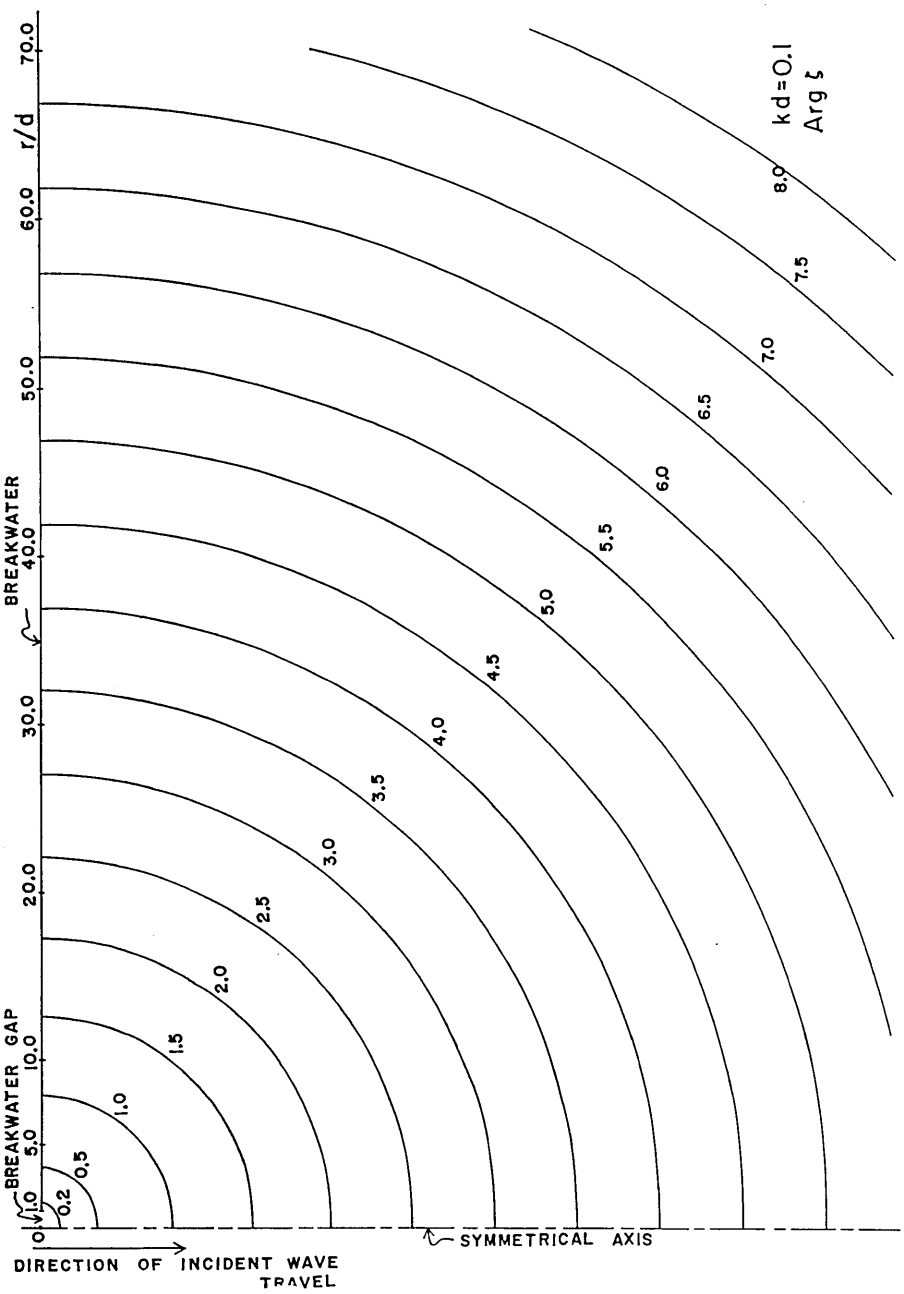

Fig. 37. Overall variation of arg ζ in the backward sea of a breakwater for a specified value $kd=0.1$. (The stated values in the figure denote arg ζ. Since the variation is symmetric for the straight line perpendicular to a breakwater wing passing through the center of a breakwater gap, only the right-hand figure is depicted. The above figure is based on the theory of the 5th approximation.)

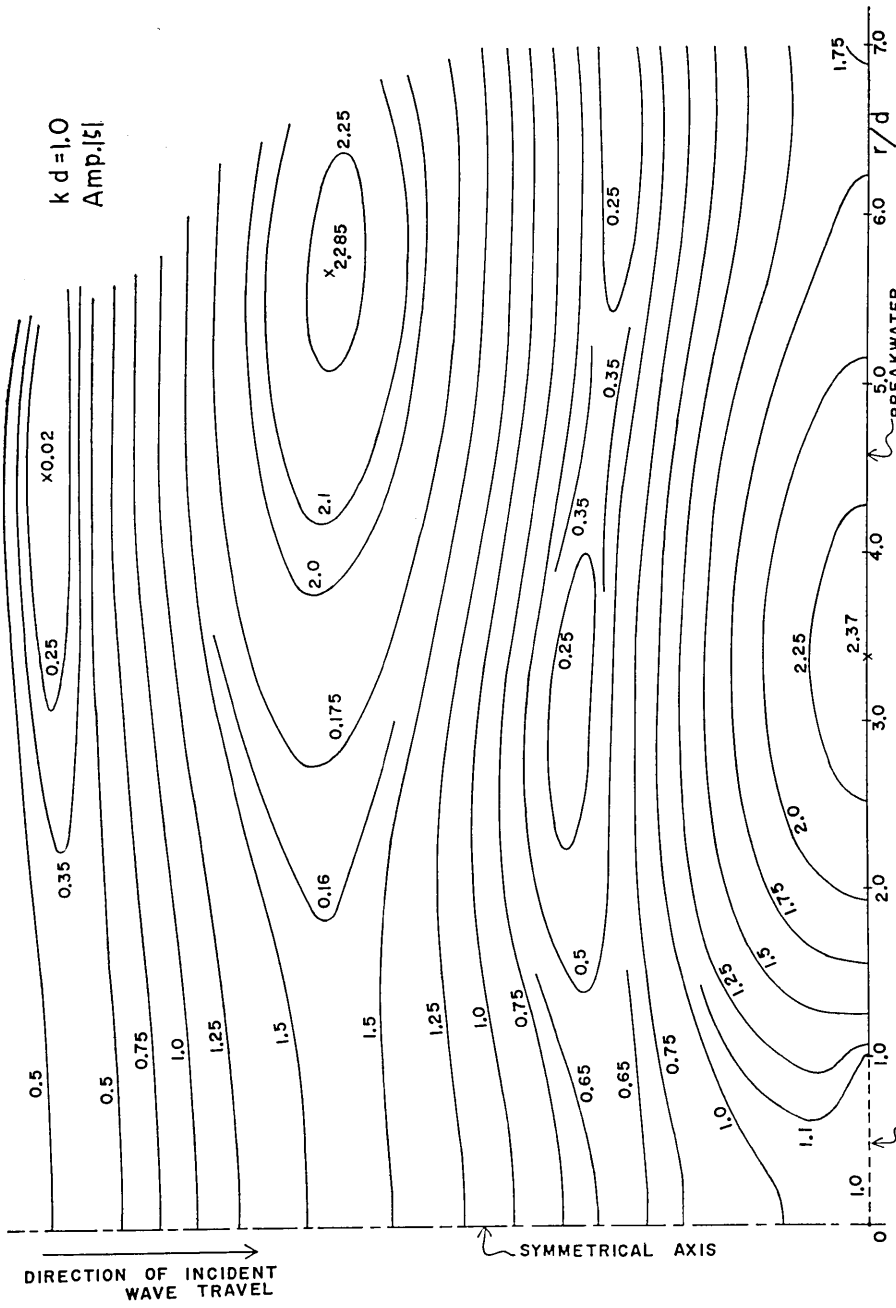

Fig. 38. Overall variation of amplitude $|\zeta|$ in the forward sea of a breakwater for a specified parameter $kd=1.0$. (The stated values in the figure denote those of $|\zeta|$ normalized by the amplitude of the incident waves ($=1.0$). Since the variation is symmetric for the straight line perpendicular to a breakwater wing passing through the center of a breakwater gap, only the right-hand figure is depicted. The above figure is depicted on the basis of the theory of the 9th approximation.)

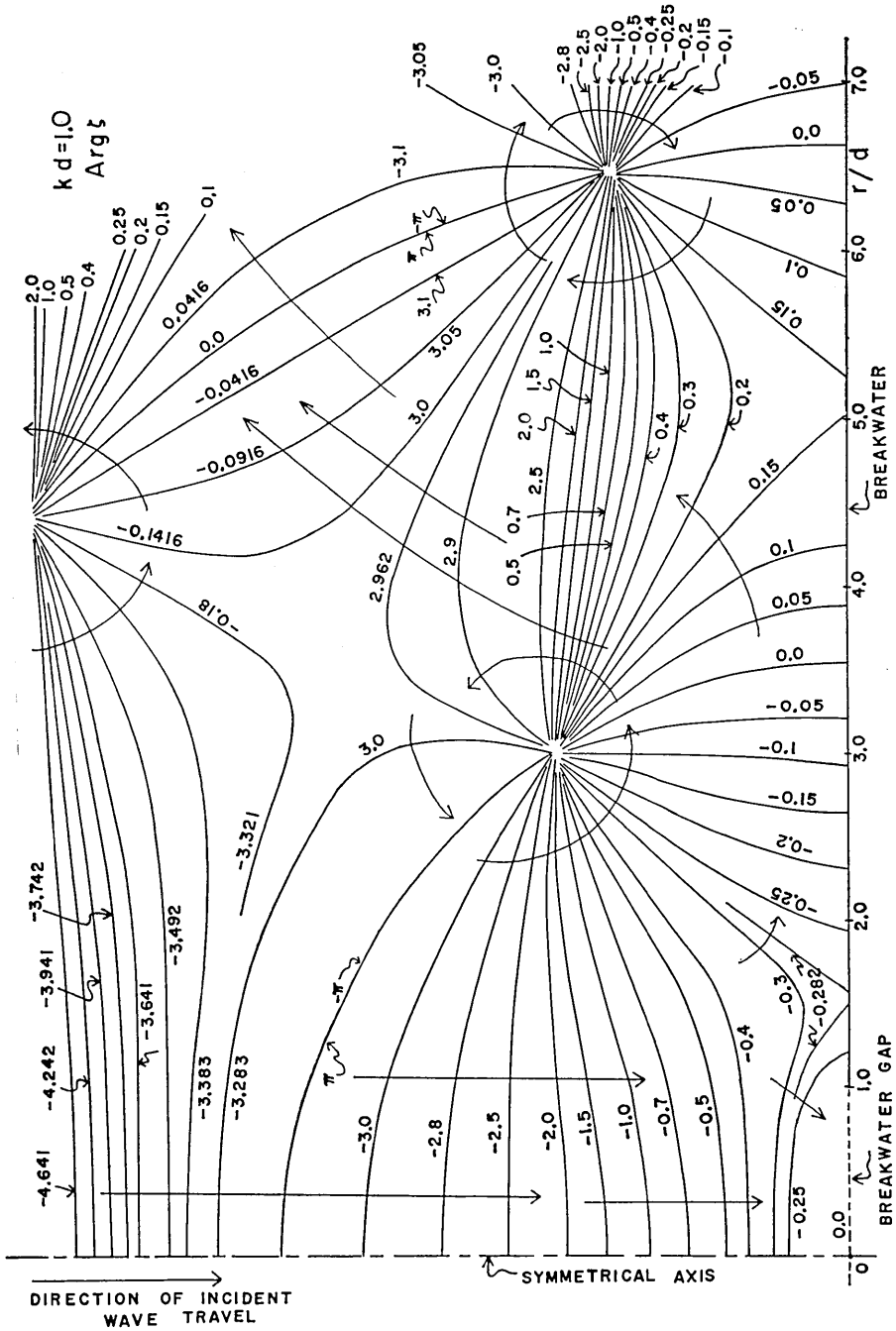

Fig. 39. Overall variation of arg ζ in the forward sea of a breakwater for a specified value $kd=1.0$. (The stated values in the figure denote arg ζ. Since the variation is symmetric for the straight line perpendicular to a breakwater wing passing through the center of a breakwater gap, only the right-hand figure is retained. The above figure is depicted based on the theory of the 9th approximation.)

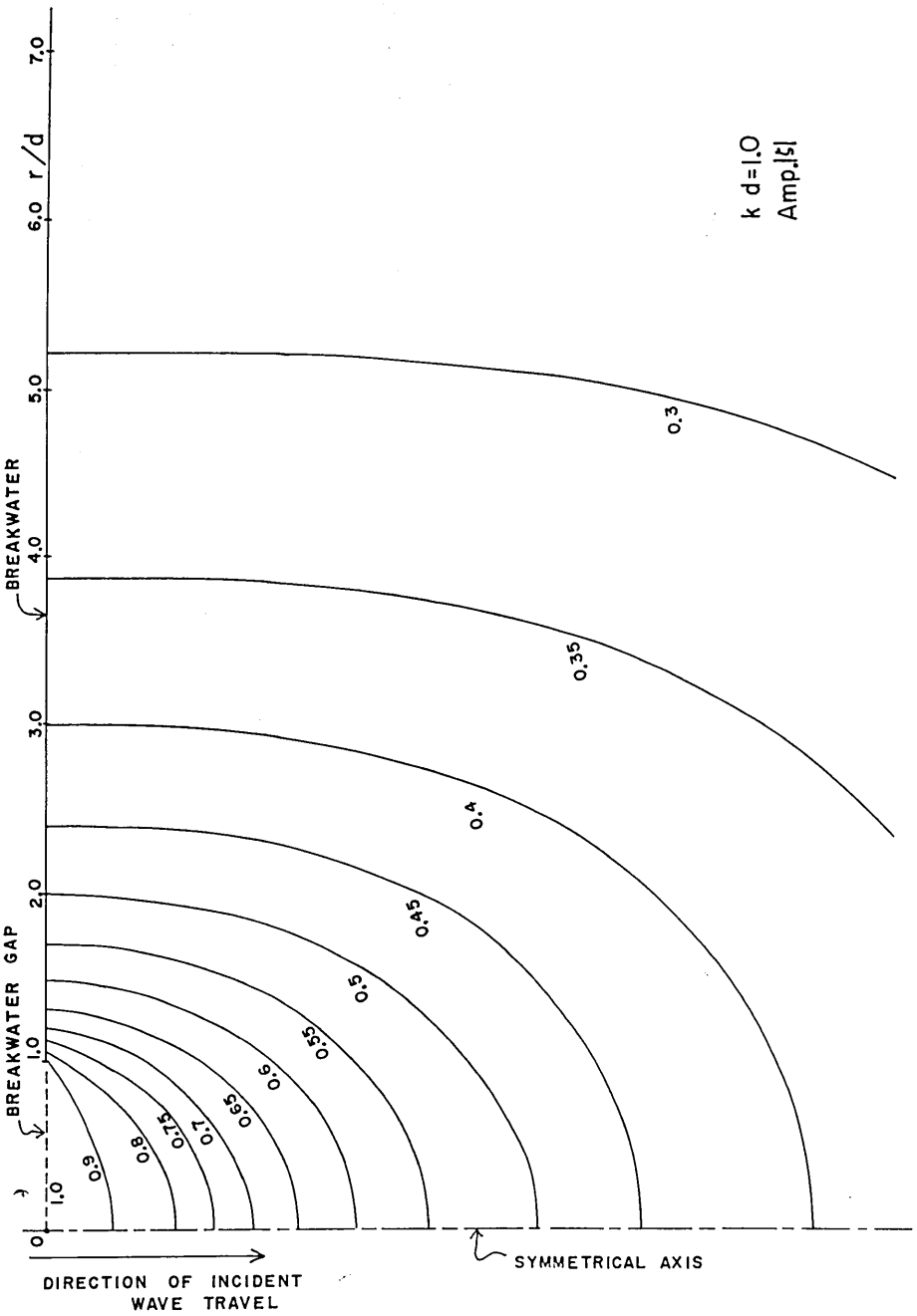

Fig. 40. Overall variation of amplitude $|\zeta|$ in the backward sea of a breakwater for a specified parameter $kd=1.0$. (The stated values in the figure denote those of $|\zeta|$ normalized by the amplitude of the incident waves ($=1.0$). Since the variation is symmetric for the straight line perpendicular to a breakwater wing passing through a center of breakwater gap, only the right-hand figure is retained. The above figure is depicted based on the theory of the 9th approximation.)

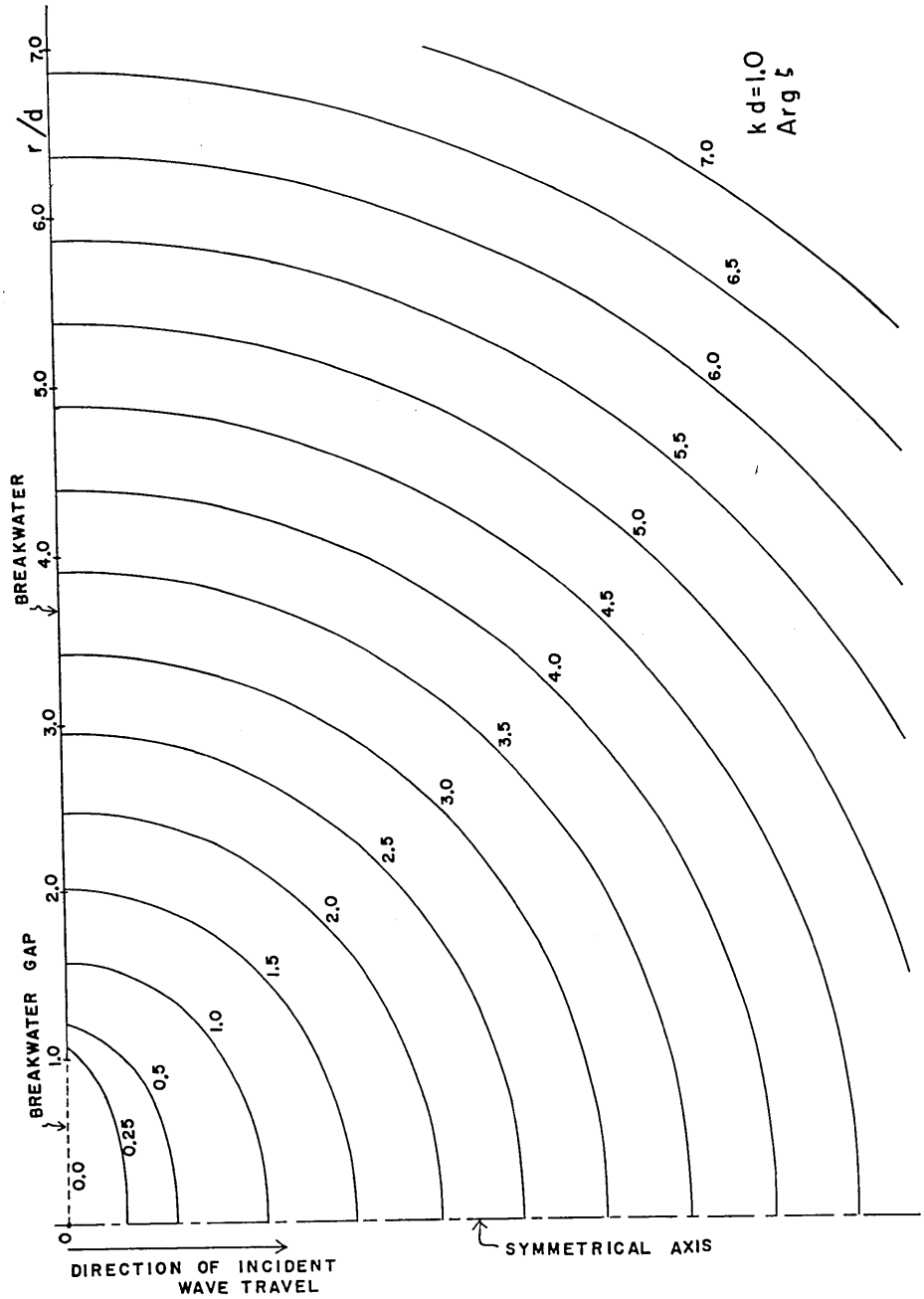

Fig. 41. Overall variation of arg ζ in the backward sea of a breakwater for a specified value $kd=1.0$. (The stated values in the figure denote those of arg ζ. Since the variation is symmetric for the straight line perpendicular to a breakwater wing passing through a center of breakwater gap, only the right-hand figure is retained. The above figure is depicted based on the theory of the 9th approximation.)

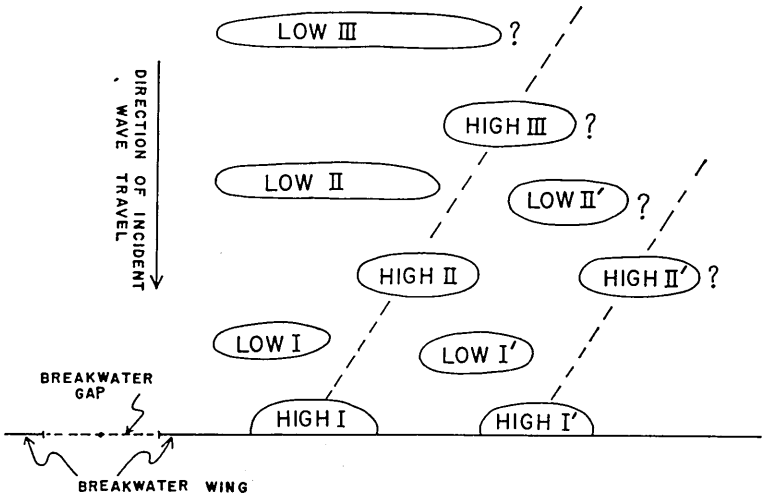

Fig. 42. Figurative explanation of variation of wave height in the forward waters of a breakwater.

forward waters of a breakwater (Figs. 34 and 38), the isolines of the amplitude for $kd=0.1$ (small kd) run comparatively parallel to the wall of a breakwater as compared with those for $kd=1.0$ (large kd). Such a trend might be considered to prevail for other values of kd.

The cause of generation of the afore-mentioned high waves is an occurrence of reflected waves accompanying rotating waves in the nearby part of a breakwater, which will be ascertained later in the variation of phase.

In Figs. 34 and 38, the isolines of the amplitude in the neighbouring regions of the domains D_1 and D_2 (see Fig. 1) were interpolated appropriately,***) because the deficiency of degree of the approximation of used theory causes insignificant irregularity in these regions, of which mention has already been made in Section *3,1. (Check of Convergence)*. In order to make detailed discussions of the behaviors of the waves in these regions, an improvement of the approximated theory, therefore, is required.

In the next section, we turn our attention to the variation of phase in the forward sea.

In Figs. 35 and 39 (the former is relevant to $kd=0.1$ and the latter to $kd=1.0$), rotating waves accompanied by the waves reflected at the

***) This convention is followed in the figures showing the overall variations of the waves around a breakwater (Figs. 35, 36, 37, 39, 40 and 41).

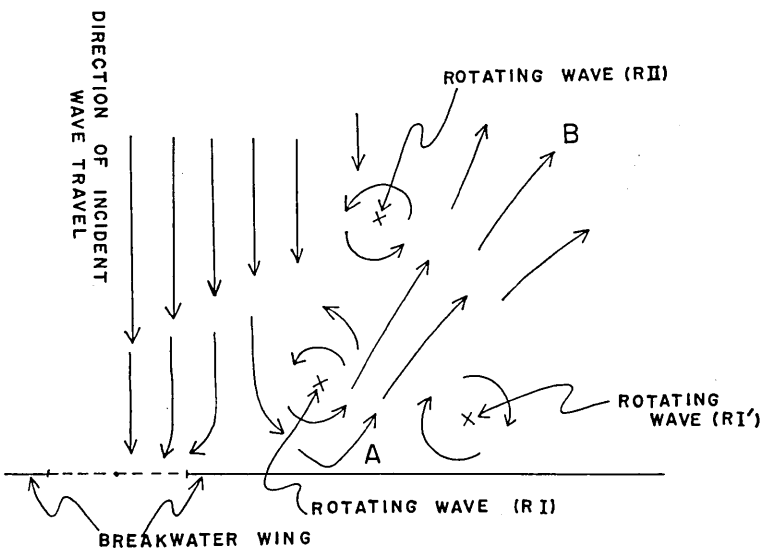

Fig. 43. Figurative explanation of variation of phase in the forward sea of a breakwater.

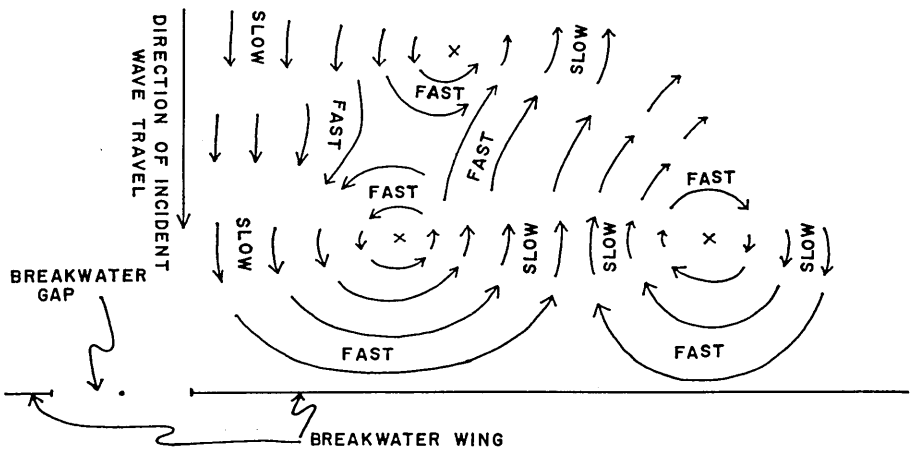

Fig. 44. Phase variation of waves in the forward sea of a breakwater.

breakwater are seen. These behaviors are figuratively illustrated in Fig. 43. As shematically shown in Fig. 43, the incident waves in front of the entrance of a breakwater advance toward the breakwater to penetrate partly into the inside of a breakwater through the entrance and to divert partly toward the nearby part of the wall facing the open

sea, the latter of which are reflected to the outer sea producing high waves near the wall (exceeding twice the amplitude of the invading waves). The waves reflected in such a way are propagated in an oblique direction instead of the counter-direction of the invading waves (to the direction from A to B in Fig. 43). In bordering regions of the incident and reflected waves, a row of rotating waves (RI, RII and so on) is then produced as a complementary flow of the above two kinds of waves. And also, outside the reflected waves, rotating waves (stated by RI' in Fig. 43) appear as a counter-flow of the reflected waves ($\overrightarrow{AB}$ in Fig. 43). A sequence of such rotating waves, therefore, might be predicted in the outer region of the depicted figure. From Figs. 35 and 39, the rotating waves are found to rotate with a period of the incident waves (the variation of the gyrating waves closes with a phase of 2π). Further, as shown figuratively in Fig. 44, a velocity of whirling waves is slower in propagation to the direction perpendicular to a breakwater, while being faster along the direction of a breakwater.

Our attention is next turned to the behaviors of the waves in the backward sea of a breakwater for specified parameters $kd=0.1$ and 1.0.

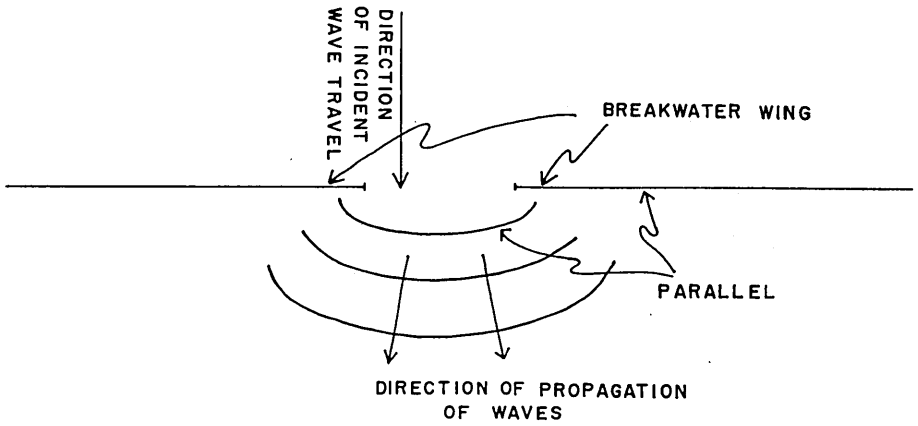

Fig. 45. Figurative explanation of phase variation of waves in the leeward of a breakwater gap.

According to Figs. 36 and 40, as already noted in Section *3,2* (*Variations of Amplitude in Typical Directions*), definite directivity of the waves is found for large kd (corresponding to the waves of small wavelength as compared with a breadth of the entrance of a breakwater),

while no appreciable directivity is seen for the waves of small kd (corresponding to long wave-length). As seen in Fig. 40 (for $kd=1.0$), a gradient of the amplitude of the waves is the greatest along the wall of a breakwater to diminish gradually in magnitude as the direction of the propagation is turned to that of incidence of the waves. Referring to Fig. 41 (the figure concerning the variation of phase for $kd=1.0$), the isolines of phase in the nearby region of the mouth of a breakwater run relatively parallel to the wall of a breakwater (see Fig. 45). This implies that the propagation of waves is more favoured in the direction of incidence of the waves than in other directions, which is consistent with the directivity of the variation of amplitude (Fig. 40). As the waves advance, such directivity of phase gradually disappears as a result of divergence of the waves due to the diffraction (when $r=4d$ in Fig. 41, with the isoline of phase running almost in circular form having the center in $r=0$). On the contrary, when $kd=0.1$, an explicit directivity of phase is not found (refer to Fig. 37). The waves which penetrated through the entrance of a breakwater are propagated uniformly to all the directions.

4. Complementary Remarks

As far as a mechanism of generation of high waves near the gap of a breakwater is concerned, a definite explanation has not been given in this paper. It is probable that a high wave denoted by "HIGH I" in Fig. 42 is produced as the result of coupling of the waves reflected and diffracted at the two breakwater wings. In order to examine this possibility, the numerical calculation of the theory of the waves in front of a single breakwater wing is useful, which is established by Sommerfeld[14]. This calculation is reserved for a future paper.

In the experiment made by Putnam and Arthur[15] or Blue and Johnson[16], the used approximated theory is considered to be useful for the waves of relatively short wave-length. In Blue and Johnson's approximated theory, they estimated that, when a gap of a breakwater is as great as 2λ (λ: a wave-length of the incident waves), a departure of the approximated theory from a rigorous one is small. As the ratio of a breakwater gap and a wave-length of the incident waves ($2d/\lambda$) begins

14) G. WOLFSOHN, *loc. cit.*, 5).
15) J. A. PUTNAM, and R. S. ARTHUR, *loc. cit.*, 2).
16) Frank L. BLUE, Jr. and J. W. JOHNSON, *loc. cit.*, 4).

to be small, the coupling effect of both breakwater wings upon the waves becomes so great that the approximated theories devised by the above-mentioned authors cannot be applied to such a problem. For the waves of a large wave-length as compared with a width of a breakwater, the procedure developed in this purview is powerful. In the subsequent papers, the difference of the results obtained by the approximated theory (devised by Putnam and Arthur or Blue and Johnson) and the rigorous theory (developed by the author) will be examined.

---

8. 防波堤のまわりにおける長波 (垂直入射の場合) [I]

地震研究所　桃　井　高　夫

本報告において防波堤のまわりの長波に関する理論が *buffer domain* の方法を用いて導入され，電子計算機を用いて防波堤の近傍における長波の状態が解明されている．

得られた結果の中で最も著しい点は，防波堤の入口の近傍に特種な反射波が現われることである．反射波は防波堤の入口近傍に波高の高い部分 (その波高は入射波の波高の 2 倍をこえている) を作り，更にこの反射波の両側には回転する波が (補流として) 現われる．
